Modeling Integrated Power and Transportation Systems: Impacts of Power-to-Gas on the Deep Decarbonization

Bo Li, *Student Member, IEEE*, Minyou Chen, *Senior Member, IEEE*, Ziming Ma, *Member, IEEE*, Gang He, Wei Dai, *Member, IEEE*, Dongran Liu, Chi Zhang, *Student Member, IEEE*, and Haiwang Zhong, *Senior Member, IEEE*

***Abstract*—The deployment of renewable energy sources, power-to-gas (P2G) systems, and zero-emission vehicles provide a synergistic opportunity to accelerate the decarbonization of both power and transportation system. This article investigates the prospects of implementing hydrogen P2G technology in coupling the power system and the transportation system. A novel coordinated long-term planning model of integrated power and transportation system (IPTS) at the regional scale is proposed to simulate the power system balance and travel demand balance simultaneously, while subject to a series of constraints, such as CO2 emission constraints. IPTS of Texas was investigated considering various CO2 emission cap scenarios. Results show unique decarbonization trajectories of the proposed coordinated planning model, in which IPTS prefers to decarbonizing the power sector firstly. When the power system reaches ultralow carbon intensity, the IPTS then focuses on the road transportation system decarbonization. The results show that with the P2G system, IPTS of Texas could achieve 100% CO2 emission reductions (relative 2018 emissions level) by adding a combination of approximately 143.5 GW of wind, 50 GW of solar PV, and 40 GW of P2G systems with 2.5% renewables curtailment. The integration of the P2G system can produce hydrogen by use of surplus RES generation to meet hydrogen demand of Fuel cell electric vehicles (FCEVs) and to meet multiday electricity supply imbalances.**

***Index Terms*—Capacity expansion, fuel cell electric vehicle, integrated power and transportation system, power-to-gas technology, smart charging.**

Manuscript received February 28, 2021; revised August 25, 2021; accepted September 26, 2021. Date of publication September 30, 2021; date of current version March 20, 2022. This work was supported by Project supported by Graduate Scientific Research and Innovation Foundation of Chongqing under Grant CYB19022. *(Corresponding authors: Minyou Chen; Haiwang Zhong.)*

Bo Li is with the School of Electrical Engineering, Chongqing University, Chongqing 400044, China, and also with the Renewable and Appropriate Energy Laboratory, University of California, Berkeley, CA 94720 USA (e-mail: boli9301@163.com).

Minyou Chen and Chi Zhang are with the School of Electrical Engineering, Chongqing University, Chongqing 400044, China (e-mail: minyouchen@cqu.edu.cn; wsxbjx@163.com).

Ziming Ma is with the National Power Dispatching and Control Center, Beijing 100031, China (e-mail: mzm_thu@foxmail.com).

Gang He is with the Department of Technology and Society, College of Engineering and Applied Sciences, Stony Brook University, Stony Brook, NY 11794 USA (e-mail: gang.he@stonybrook.edu).

Wei Dai is with the Department of Electrical Engineering, Guangxi University, Nanning 530004, China (e-mail: weidai@gxu.edu.cn).

Dongran Liu is with the School of Economics and Management, North China Electric Power University, Beijing 102206, China (e-mail: 1182106008@ncepu.edu.cn).

Haiwang Zhong is with the Department of Electrical Engineering, Tsinghua University, Beijing 100084, China, and also with the State Key Lab of Control and Simulation of Power Systems and Generation Equipment, Tsinghua University, Beijing 100084, China (e-mail: zhonghw@tsinghua.edu.cn).

Color versions of one or more figures in this article are available at https://doi.org/10.1109/TIA.2021.3116916.

Digital Object Identifier 10.1109/TIA.2021.3116916

Nomenclature

A. Abbreviations

BEV	Battery electric vehicle.
ICEV	Internal combustion engine vehicle.
FCEV	Fuel cell electric vehicle.
HRS	Hydrogen refueling station.
P2G	Power-to-gas.
P2P	Power-to-gas-to-power.
BESS	Battery energy storage system.
IPTS	Integrated power and transportation system.
O&M	Operational and maintenance costs.
EVSE	Electric vehicle supporting equipment.
H2	Hydrogen.

B. Indices

z	Index of load zone.
g	Index of generation technology.
f	Index of fuel type.
l	Index of transmission line.
v	Index of vehicle type.
s	Index of storage technology.
t	Index of hour.
r	Index of pipeline type.
P	Index of parking locations of vehicles.
Ψ_z^F	Index set of fossil-fuel-fired generators in load zone z.
Ψ_z^R	Index set of renewable energy generators in load zone z.
Ψ_z^{BEV}	Index set of BEVs in load zone z.
Ψ_z^{FCEV}	Index set of FCEVs in load zone z.
Ψ_z^{ICV}	Index set of ICEVs in load zone z.
Ψ_z^{ES}	Index set of energy storages in load zone z.
ϕ^{BEV}	Index set of BEVs.
ϕ^{ICEV}	Index set of ICEVs.
L_z^{in}	Index set of transmission lines whose flows are directed into load zone z.

L_z^{out} Index set of transmission lines whose flows are out of load zone *z*.

C. Variables

$P^{z,g,t}$ Electric power output of generators [MW].
$U_{\text{on}}^{z,g,t}$ Commitment capacity of generators [MW].
$N_{z,v}$ The population of vehicle category [unit].
G_{HRS}^{z} Capacity of hydrogen refueling station (HRS) [kg H_2/day].
$G_{\text{ES,E}}^{s}$ Energy- related capacity of storage technology [MWh].
$G_{\text{ES,P}}^{s}$ Power- related capacity of storage technology [MW].
$P_{EV}^{\text{z,v,t}}$ Electricity charging power of electric vehicle category *v* in load zone *z* at hour *t* [MW].
$S_{\text{on}}^{Z,g,t}$ Additional capacity to startup of generators [MW].
$D_{\text{down}}^{Z,g,t}$ Additional capacity to shutdown of generators [MW].
$P_{\text{up}}^{z,g,t}, P_{\text{down}}^{z,g,t}$ Spinning up/ down reserves of generators [MW/hour].
$P_{Dis,\text{up}}^{\text{z,s,t}}$ Spinning up reserves of storage category *s* [MW/hour].
$P_{Dis,\text{down}}^{\text{z,s,t}}$ Spinning down reserves of storage category *s* [MW/hour].
$G^{z,g}$ Total generation capacity of generators [MW].
$D_{\text{Pipe}}^{z,r}$, Diameter of gas pipeline type [m].
$F_{l,t}$ Power flow of transmission line *l*.
I_{cap}^{l} Total transmission capacity of transmission line *l*.

D. Parameters

CRF Capital recovery factor.
c_{inv}^{g} Investment cost of generators [$/MW].
$c_{\text{L,cap}}^{l}$ Investment cost of transmission lines [$/MW].
c_{FOM}^{g} Fixed O&M cost of generators [$/MW-year].
$c_{\text{L,FOM}}^{l}$ Fixed O&M cost of transmission line [$/MW-year].
c_{VOM}^{g} Variable O&M cost of generators [$/MWh].
h^{g} Heat rate of generators [MMBtu/MWh].
c_{fuel}^{f} Fuel cost of fuel type [$/MMBtu].
c_{on}^{g} Start-up cost of generators [$/MW].
$c_{\text{veh,PC}}^{v}$ The purchase cost of vehicle category [$/vehicle].
$c_{\text{veh,IF}}^{v}$ The investment cost of charging piles of vehicle category [$/vehicle].
$c_{\text{veh,FOM}}^{v}$ Fixed O&M cost of vehicle category [$/vehicle-year].
c_{HRS} Investment cost of HRS [$/kg H_2].
AVDT_v Annual vehicle distance travel of vehicle category [km/vehicle-annual].
fcr_v Fuel economy of vehicle category *v* ([gallon gasoline/km] for ICEVs, [kWh/km] for BEVs, [kg H_2/km] for FCEVs).
$c_{\text{inv,E}}^{s}$ Energy-related capital costs of storage technology [$/MWh].
$c_{\text{inv,P}}^{s}$ Power- related capital costs of storage technology [$/MW].
$c_{\text{Pipe}}^{z,r}$ Investment cost of pipelines type.
$d_{\text{pipe}}^{z,r}$ Transmission distance of pipelines.
$f_{\text{Pipe}}(D_{\text{Pipe}}^{z,r})$ $0.064 \cdot D_{\text{Pipe}}^{z,r} - 0.2799$ is a pipeline cost calculation equation ($/km) [1].
$c_{\text{ES, EFOM}}^{z}$ Fixed O&M cost of storage technology [$/MWh-year].
$c_{\text{ES. VOM}}^{z}$ Variable operational cost of storage technology [$/MWh].
dh_{ES}^{z} Maximum discharging hours of energy storage in rated generation capacity.
$\overline{G^{z,g}}$ Cumulative generation capacity upper of generators.
$\overline{N_{z,v}}$ Cumulative vehicle fleet population upper.
$\overline{I_{\text{cap}}^{l}}$ Cumulative capacity upper of transmission lines.
Δt Duration of a time interval [1 hour in this article].
$D^{z,t}$ Electricity demand of load zone z at hour t [MW].
$cf^{z,g,t}$ The hourly capacity factors for generator g hour *t* (1 for thermal generators).
$d_{\text{min}}^{z,g}$ The minimum dispatch fraction (minimum load) of the committed capacity for generation technology i.
$RU^{z,g}, RD^{z \cdot g}$ Ramp-up/ down ratio limitation of generation technology *g*.
$T_{\text{on}}^{z,g}, T_{\text{off}}^{z,g}$ Minimum on time/ off-line time of generation technology *g*.
$\beta^{z,g}$ Capacity credit of generation technologies [%].
$R_{\text{load}}^{\text{up}}, R_{\text{load}}^{\text{down}}$ Spinning up/ down ratio requirement related to electricity demand [%].
$R_{\text{RES}}^{\text{up}}, R_{\text{RES}}^{\text{down}}$ Spinning up/ down reserve ratio requirement related to renewable generation output [%].
e_{emi}^{f} CO_2 emission per unit energy consumption of fuel category *f* [kg CO_2/MMBtu]. 93.28 for coal and 53.06 for natural gas.
EM_{CO2} Total carbon emission allowance for IPTS [ton CO_2/year].
$E_{\text{ES}}^{z,s,t}$ Energy storage level at hour *t* [MWh].
$\eta_{\text{in}}^{s}, \eta_{\text{out}}^{s}$ Charging/discharging efficiency of storage technology z [%].
$\underline{\varepsilon_{\text{ES}}}, \overline{\varepsilon_{\text{ES}}}$ Lower/upper energy limit for storage technology z. [%].
τ $\text{ceil}((G_{\text{ES,E}}^{z}/G_{\text{ES,P}}^{z})/24)$ That rounds element of τ to the nearest integer greater than or equal to that element.
$H_{\text{Dis}}^{z,s,t}$ Discharging power of P2P systems to HRSs through pipelines or truck trailers [MW].
η_{pipe}^{z} Transmission efficiency of pipelines in load zone z [%].
fe_{H2} Low heating value of H_2 [33.3 kWh/kg].
$f_{\text{fr}}(G_{\text{Pipe}}^{z,r})$ $\pi(G_{\text{Pipe}}^{r}/2)^2 \cdot vel_{H2} \cdot den_{H2} \cdot 3600,$ which is the function to calculate maximum flow rate of pipelines [kg H_2/hour].
vel_{H2} H_2 velocity [m/s].

den_{H2}	H_2 density [kg/m^3].
$Q_{\mathrm{FCEV}}^{\mathrm{z,v,t}}$	H_2 refueling rate of FCEVs [kg H_2/hour].
$Q_{\mathrm{HRS}}^{z,t}$	Hydrogen storage level of HRSs at hour *t*.
$\underline{\varepsilon_{\mathrm{HRS}}}, \overline{\varepsilon_{\mathrm{HRS}}}$	Minimum/ maximum levels of residual energy in HRSs.
$\mathrm{EVDh}_{\mathrm{EV}}^{\mathrm{z,v,t}}$	Hourly zone demand of BEV fleet [kW].
$E_{\mathrm{EV}}^{\mathrm{z,v,t}}$	Energy capacity level of vehicle category *v* in load zone *z* at hour *t* ([kWh] for BEVs and [kg H_2] for FCEVs).
η_{EV}^{v}	Charging/refueling efficiency of vehicle category *v* [%].
$\mathrm{VDT}_{\mathrm{EV}}^{\mathrm{v}}$	Daily vehicle distance drive of vehicle category *v* [km/day].
$\mathrm{PVDT}_{\mathrm{EV}}^{\mathrm{z,v,t}}$	Percentage of daily vehicle distance traveled of vehicles [%].
$\underline{\varepsilon_{\mathrm{EV}}}, \overline{\varepsilon_{\mathrm{EV}}}$	Minimum/ maximum levels of residual energy in all vehicle categories. [%].
$Ener\mathrm{EV}_{\mathrm{EV}}^{v}$	Rated energy capacity of vehicle category v ([kWh] for BEVs, [kg H_2] for FCEVs).
$Cap\mathrm{EVSE}_{\mathrm{EV}}^{v,p}$	Rated charging power of EVSE in dwell location *p* for vehicle category *v* [kW].
$ProLoc_{\mathrm{EV}}^{v,p,t}$	Percentage of vehicle category *v* parking in location *p* in time *t* [%].
$\mathrm{CPEV}_{\mathrm{EV}}^{v,p}$	The number of EVSE to EV ratio in location *p.*
α	The number of days for a vehicle can drive in full SOC.

I. Introduction

DECARBONIZATION of the energy system requires urgent actions on all sectors. Power and transportation sectors remain the world's major obstacles for effective CO2 emission reduction [2]. Increasing variable renewable energy (VRE) like wind and solar will bring strong challenges that ensure continuous balances between electricity generation and consumption on both short-term and long-term scales [3]. For instance, outputs of VRE are uncertain and exhibit variable diurnal and seasonal patterns, leading to more frequent net load fluctuations and more requirement for flexibility in the power system [4]. Besides, BEVs and FCEVs are main options to decarbonize transportation sectors in the future [5]. The both options highly rely on electricity from power generation or hydrogen fuel generated from electrolysis, which are more closely linked to the power system [6]. Amid these trends, power generation and mobility are expected to interweave more and more, leading to an integrated energy system. Transportation electrification would increase overall electricity demand in the power system, leading to more generation capacity, transmission and distribution capacity [6], and CO_2 emissions for power systems. The importance of integrating power and transportation sectors is growing, especially under the rising amount of BEVs and FCEVs [7], and climate policies. Previous studies have examined at least three important problems related to the coupled power and transportation systems. First, many studies have investigated the integrated charging power profiles of BEVs into the power system operation both temporally and spatially. These studies usually formulate power and transportation system models, in which the former is modeled as an optimal power flow problem, and the latter is modeled as a flexible load that can be dispatched by either time-of-use electricity prices [8] or system operators directly [9], achieving economic dispatch while meeting a series security constraints [10], [11]. Past studies indicate that vehicle-grid integration can provide the power system with substantial flexibility [12], reducing peak demand [13], load balancing [7], frequency regulation, reducing curtailment of renewable generation [12], and participating in ancillary services [11]. BEV diversity (vehicle types, use patterns, and charging options), accessibility of charging infrastructures, time-of-use (TOU) tariffs, generation mixes, and network structures play important roles in integrating EV charging load into the power system with an increasing electrified fleet of vehicles. The second related body of research addresses the power system planning problem considering BEV charging demand, i.e., minimize the total cost of the power system. The mobility demand is usually regarded as an exogenous parameter in the power system capacity expansion model through scenario analysis to explore the effects of EVs on the power system operation and planning [6], [14], [15]. In [6] and [16], a power system capacity expansion model integrated larger-scale EVs is presented. The results indicate that a necessary increase in electricity generation capacity and transmission capacity occurred due to transportation electrification in U.K. and China. Meanwhile, TOU tariffs and smart charging strategy of EVs enable further reduce capacity and transmission requirements, national peak demand, and so on. Third, vehicle population mix can be optimized coordinately with the generation capacity of the power system to achieve deep decarbonization simultaneously. Brozynski and Leibowicz [17] developed an energy system optimization model for unban-scale decarbonization involving power and transportation sectors. The optimal decarbonization pathway proceeds through two distinct stages, first reducing power sector emissions, then electrifying transportation. Colbertaldo *et al.* [18] compared a set of medium- and long-term scenarios for power generation and road transport in Italy, indicating that power-to-gas technology is expected to be a key role in interacting power and transportation systems.

Moreover, very high penetrations of renewable energy sources (RES) facilitate the deployment of energy storage to reduce RES curtailment and help to shift the energy imbalance during multiday periods [3], [4]. The energy storage technologies have different physical characteristics (e.g., discharge durations, round-trip efficiencies) and grid applications (load-shifting, frequency regulation). The most studied energy storage technologies are BESS and P2G. Currently, the cost of energy storage is a major obstacle to their deployment and application in the power grid. However, dramatic cost reductions in BESS in the future will show its significant potential in balancing grid power imbalance [19]. P2G is based on the conversion of electrical power to gaseous fuel, especially power to hydrogen via electrolysis plus hydrogen storage. P2G can couple the power sector with other sectors (e.g., mobility) and, thus, contribute to their decarbonization of both sectors. If hydrogen fuel is reused to produce electricity via either fuel cells or gas turbines, it refers to P2P technology

[20]. P2G/P2P system can store electricity during low demand periods and supply energy during high demand periods, enabling to capture variations of VRE generation. P2G/P2P offers the advantage of multiple possible hydrogen use pathways, among others: direct use as fuel for transportation and reconversion to electricity via fuel cells [21]. Towards 100% renewable electricity grid could require massive storage technologies (including pumped hydro storage, compressed air energy storage, and hydrogen storage system) in different time scales (hourly, daily, and seasonally) [22]. Many studies have been devoted to the techno-economic assessment for hydrogen storage technologies focusing on hydrogen production [23], delivery [24], and storage [25]. However, there is a lack of understanding of the value of P2G/P2P technologies to facilitate sector coupling, i.e., connecting and integrating different applications such as transportation and power generation, to stabilize the supply and demand of energy in the integrated energy system.

Thus, there is a need to coordinate optimize the operation and planning of IPTS to affordable deep decarbonization outcomes. Current studies related to IPTS decarbonization pathways have two major limitations. First, these works have little research on coordinate planning between the power and transportation systems, as the number of BEVs or the share of BEVs in the total number of vehicles is usually regarded as an exogenous parameter. Moreover, transportation sector demand is simplified without considering drive characteristic differences and EVSE requirements in the vehicle category, as light-duty vehicles and heavy-duty vehicles have different drive characteristics. Second, models cannot effectively model the role of P2G/P2P in integrating power and transportation system to allow for deep decarbonization of IPTS through the excess RES generation. Including operation constraints and capital costs of hydrogen delivery and hydrogen refueling station allows for a more realistic representation of the operation and planning process, the ability of hydrogen storage technology to benefit from providing transportation fuel and generation fuel, which is of particular importance on the high renewable power systems, and more accurate characterization of P2G/P2P operation parameters.

Therefore, a coordinated planning model for decarbonizing IPTS with P2G technology is proposed to understand better the role of P2G system in deep decarbonization of IPTS. The network-constraint hourly generation dispatch model and hourly travel and energy demand of vehicles are considered. This article investigates the large-scale, low-carbon transition towards higher penetration of RES and zero-emission vehicles for IPTS at regional scale. This article focuses on the optimal installed capacity mix, energy storage capacity, and vehicle category population in Texas in 2018, under different CO_2 emission cap scenarios.

The main contributions of this article are summarized as follows.

1) A novel coordinated planning model of IPTS is proposed for the optimized investment and operation of power and transportation system. The model effectively reflects the coordinated decarbonization trajectories of IPTS.
2) The hourly charging/refueling demand of different types of zero-emission vehicles (BEVs and FCEVs) considering vehicle characteristics and driving characteristics is established. It allows different vehicle types with different fuel types to be integrated into IPTS to effectively model road transportation systems.
3) The P2G technology is introduced into the IPTS, and the processes of hydrogen production, storage, and delivery to realize multisectors coupling are designed in detail.
4) The IPTS test simulation in Texas considering power dispatch and transmission network constraints is modeled to reflect the possible evolution of IPTS in different decarbonization pathways.

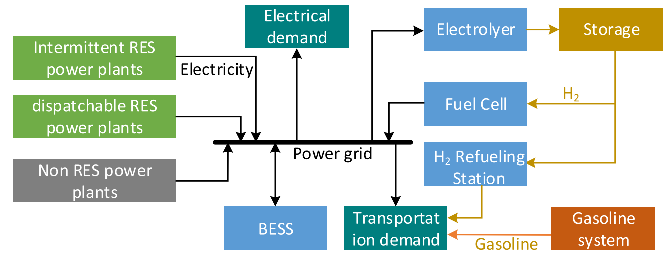

Fig. 1. Schematic of the integrated power and transportation sector structure.

The rest of this article is organized as follows. The framework of the proposed integrated energy system is presented in Section II. Section III describes the proposed planning tool for integrated power and transportation system. Section IV presents data and scenario definitions. The simulation results are discussed in Section V. Finally, Section VI concludes this article.

II. Framework

A. Integrated Power and Transportation System

The proposed IPTS structure based on P2G systems is shown in Fig. 1. The power system includes RES power plants (e.g., wind, solar PV, and hydropower), thermal power plants (e.g., coal, natural gas, nuclear, and biomass), energy storage system (e.g., BESS, P2G system), and electricity transmission networks. The road transportation system includes different fuel and vehicle types of vehicles (e.g., ICEVs, BEVs, FCEVs, passenger vehicles, and trucks) and charging/refueling infrastructures (e.g., electricity charging stations and HRS). The P2G system is connected to power and transportation systems, where the P2G system includes P2G units (e.g., water electrolyzer), gas to power units (e.g., gas turbine and fuel cell), gas wells, and gas delivery network.

This article considers the deployment of renewable electricity supply, energy storage technologies, and alternative vehicle technologies to investigate the influence of P2G systems on IPTS decarbonization. A linear programming model that simultaneously optimizes electricity and transportation system planning and operation for a single year is formulated, with a temporal resolution of one hour.

B. Power System

In the power system, the electricity is produced by power plants and then transported from energy sources to the load through the electricity transmission network. The electricity network constraint is molded through the dc power flow. After P2G system is integrated into power systems, surplus renewables power can be converted to hydrogen through electrolyzers. Hydrogen can be converted into electricity through fuel cells or gas turbines to meet the electricity demand shortage. Moreover, hydrogen can be transported to the hydrogen refueling stations (HRSs) through gas delivery network to meet mobility demand. Notably, due to nonlinear characteristics of the gas pipeline networks, including compressor operation and gas flow [26], [27], gas pipeline networks in this article are assumed to be a linear input and output network, where the gas volumetric flow is the constant value determined by pipeline factors.

In the power systems, the integrated generation capacity expansion and transmission capacity expansion model are built to determine the optimal size of the energy storage systems, power generation, the hourly operation of the power system, and electricity transmission lines while meeting a series of technical and policy constraints. Short-term and long-term energy storage can be deployed. Most of the recent short-term energy storage system such as pumped hydro and lithium-ion (Li-ion), has a typical 4 h of duration at rated power. Short-term energy storage enables daily energy time shift. Long-term energy storage is considered as from 10 to 100 h of durations at rated power [28]. In this article, Li-ion batteries are considered as a typical short-term energy storage system, and hydrogen P2G systems are considered as typical long-term energy storage. The corresponding techno-economic assumptions, e.g., electricity load profiles, fossil fuel prices, technology cost, and legacy generation capacity, are provided.

C. Transportation System

The transportation system studied in this article is road transportation, where vehicles involve a variety of fuels and vehicle types. The daily travel characteristics (e.g., departure/arrive time, dwell place, dwell time, and travel purpose) are the same for the same vehicle type with different fuel types. Thus, the total energy consumptions and CO_2 emissions of vehicles with different fuel and vehicle types can be estimated by the vehicle stock, fuel consumption rates of vehicles, and the annual vehicle traveled distances. The annual energy demand of vehicles is proportional to the vehicle fleet. This assumption can prove that existing gasoline- and diesel-powered vehicles could be shifted to zero-emission vehicles to reduce CO_2 emissions without significantly changing the driving behaviors of drivers.

The daily electricity demands from BEVs are scaled up by the vehicle fleet to add to the electricity grid load, thus affecting the generation capacity and transmission capacity requirements, and operation of a power grid. There are some common charging strategies that can be utilized, such as unmanaged charging, smart charging, and OFF-peak charging strategies [10]. The electric vehicle supporting equipment (EVSE) requirements need to coordinate with BEV deployment. The vehicle-to-grid model of vehicles is beyond the scope of this article.

The hydrogen is produced by P2G system using excess renewables power to meet FCEVs hydrogen demand, thanks to possible long-term storage technologies and short refueling times. P2G system is assumed to be in each node of electricity transmission networks. FCEV supporting equipment, including HRSs and gas delivery network, are modeled to simulate hydrogen delivery dynamics in each local node. For instance, hydrogen produced by P2G system can be stored directly into hydrogen storages or transported to HRSs through local hydrogen delivery networks. The capacity requirement of HRSs needs to meet the daily refueling profiles of FCEVs.

The fossil fuel consumption of ICEVs, such as gasoline and diesel, does not have an impact on the operation of the power grid. Thus, the energy consumptions of ICEVs can be directly calculated.

The spatial resolution of daily mobility routes between typical visited locations (home, workplace, and public places) is considered in this article. Notably, the transportation network involving specific traffic flows and route choices of vehicles is beyond the scope of this article. Thus, the charging/refueling demand of vehicles occurs in each node, meaning that no detailed transportation networks.

III. Optimization Model

The proposed coplanning model of IPTS assumes that there are government administrations that can collaborate power and transportation systems to make planning and operation decisions. The main purpose of the proposed model is to investigate long-term planning and operation guidance. The combinations of capital costs and efficiency of energy storage system, CO_2 caps, and FCEVs' purchase costs drive the power and transportation sectors. The coplanning model is applied to generate and explore the future scenarios of IPTS and analyze the CO_2 emission benefits, and economic benefits of the P2G system.

A. Objective Function

The proposed model is formulated as a linear program that determines the least-cost power and transportation infrastructures combinations, vehicle population mixes, and operational schedules that satisfy electricity and mobility demands, subject to a series of technical and policy constraints

$$\min \mathrm{CRF} \cdot \left(C_{\text{Power}}^{Inv} + C_{\text{Trans}}^{Inv} + C_{\text{ES}}^{Inv}\right) + C_{\text{Power}}^{\text{Op}} + C_{\text{Trans}}^{\text{Op}} + C_{\text{ES}}^{\text{Op}} \tag{1}$$

$$C_{\text{Power}}^{Inv} = \sum_{z,g} G^{z,g} \cdot c_{inv}^{g} + \sum_{l} c_{L,\text{cap}}^{l} \cdot I_{\text{cap}}^{l} \tag{2}$$

$$C_{\text{Power}}^{\text{OP}} = \sum_{z,g,t} P^{z,g,t} \cdot h^{g} \cdot c_{\text{fuel}}^{f} \cdot \triangle t + \sum_{z,g,t} P^{z,g,t} \cdot c_{\text{VOM}}^{g} \cdot \triangle t + \sum_{z,g,t} S_{\text{on}}^{z,g,t} \cdot c_{\text{on}}^{g} + \sum_{z,g} G^{z,g} \cdot c_{\text{FOM}}^{g} + \sum_{l} c_{L,\text{FOM}}^{l} \cdot I_{\text{cap}}^{l} \tag{3}$$

$$C_{\text{Trans}}^{Inv} = \sum_{z,v} N_{z,v} \cdot c_{veh,\text{PC}}^{v} + \sum_{z,v \in \phi^{\text{BEV}}} N_{z,v} \cdot c_{veh,IF}^{v} + G_{\text{HRS}}^{z} \cdot c_{\text{HRS}} \tag{4}$$

$$C_{\text{Trans}}^{\text{OP}} = \sum_{z,v\in\phi^{\text{ICEV}}} N_{z,v}\cdot \text{AVDT}_v \cdot fcr_v \cdot c_{\text{fuel}}^{f} + \sum_{z,v} N_{z,v}\cdot c_{veh,\text{FOM}}^{v} \quad (5)$$

$$C_{\text{ES}}^{Inv} = \sum_{z,s} G_{\text{ES},E}^{z,s} c_{inv,E}^{s} + G_{\text{ES},P}^{z,s} c_{inv,P}^{s} + f_{\text{Pipe}}\left(D_{\text{Pipe}}^{z,r}\right) \cdot c_{\text{Pipe}}^{z,r}\cdot d_{\text{pipe}}^{z,r} \quad (6)$$

$$C_{\text{ES}}^{\text{OP}} = \sum_{z,s,t}\left(P_{z,s,t}^{Dis} + P_{z,s,t}^{Ch}\right)\cdot c_{\text{ES},VOM}^{s} + \sum_{z,s} G_{\text{ES},E}^{z,s}\cdot c_{\text{ES,EFOM}}^{s} \quad (7)$$

where C_{Power}^{Inv} reflects the investment cost of building new generation capacity of the total generation capacity and transmission lines. C_{Power}^{OP} is the operation and fixed O&M costs of the power system, including fuel costs, variable costs, and startup costs of generators, and fixed O&M costs of transmission lines. C_{Trans}^{Inv} represents investment cost for the transportation sector, including purchase costs and fixed O&M cost for vehicles and investment cost for charging/ refueling infrastructures. C_{Trans}^{OP} represents the operation and fixed O&M costs for the transportation sector, including fuel cost for gasoline and hydrogen delivery cost. C_{ES}^{Inv} represents the investment cost of storage systems. C_{ES}^{OP} represents the operation and fixed O&M cost of energy storage systems.

B. Investment Constraints of the IPTS

The investment constraints of generating technologies are based on the resource potential, technology development, land uses, and policy targets

$$0 \le G^{z,g} \le \overline{G^{z,g}} \quad (8)$$

$$\sum_{z,v} N_{z,v} = \overline{N_{z,v}} \quad (9)$$

$$0 \le G_{\text{ES},E}^{z,s} \le dh_{\text{ES}}^{s}\cdot G_{\text{ES},P}^{z,s} \quad (10)$$

$$0 \le I_{\text{cap}}^{l} \le \overline{I_{\text{cap}}^{l}}, \forall t, l \quad (11)$$

where (8) determines upper limit for new installed capacity of power plant *g*. For existing power plants, the generation capacity is a constant value, while the generation capacity of proposed generators is a decision variable. Equation (9) makes sure that total vehicle stock should be equal to the existing vehicle stocks. Equation (10) determines maximum discharging hours for different energy storage technologies. Equation (11) determines maximum generation capacity upper of transmission lines.

C. Operational Constraints of the Integrated Energy System

At each time step *t*, a series of operating constraints are considered. Constraint (12) ensures the power balance in each load zone, where the charging demands from BEVs are modeled as additional demand. The daily charging/refueling profiles of EVs/FCEVs are further discussed in Section III-F. Constraint (13) ensures that transmission power flows of transmission lines are within the maximum capacity

$$\sum_{g\in\Psi_z^G} P^{z,g,t} + \sum_{l\in L_z^{\text{in}}} \eta_{eff}^{l}\cdot F_{l,t} + \sum_{s\in\Psi_z^{\text{ES}}} P_{Dis}^{z,s,t} = D^{z,t} + \sum_{s\in\Psi_z^{\text{ES}}} P_{Ch}^{z,s,t} + \sum_{v\in\Psi_z^{\text{BEV}}} P_{\text{EV}}^{z,v,t} + \sum_{l\in L_z^{\text{out}}} \eta_{eff}^{l}\cdot F_{l,t} \quad (12)$$

$$-I_{\text{cap}}^{l} \le F_{l,t} \le I_{\text{cap}}^{l}, \forall t, l. \quad (13)$$

The power outputs limitation of generators formulated from constraint (14), in which the first constraint ensures that the output of thermal generators must be either $[d_{\min}^{z,g}\cdot U_{\text{on}}^{z,g,t}, U_{\text{on}}^{z,g,t}]$when online or zero when offline, and the second constraint ensures that the output of renewable energy generators cannot exceed the maximum available outputs based on forecasting capacity factors. Constraint (15) defines the relationship between the commitment level and the startup/shutdown decisions. Constraint (16) indicates that startup/shutdown decisions are limited by the maximum available output

$$\begin{cases} d_{\min}^{z,g}\cdot U_{\text{on}}^{z,g,t} \le P^{z,g,t} \le U_{\text{on}}^{z,g,t}, \forall g\in\psi_z^F \\ 0 \le P^{z,g,t} \le cf^{z,g,t}\cdot G^{z,g}, \forall g\in\psi_z^R \end{cases} \quad (14)$$

$$U_{\text{on}}^{z,g,t} - U_{\text{on}}^{z,g,t-1} = S_{\text{on}}^{z,g,t} - D_{\text{down}}^{z,g,t}, \forall g\in\psi_z^F \quad (15)$$

$$0 \le S_{\text{on}}^{z,g,t}, D_{\text{down}}^{z,g,t} \le G^{z,g}, \forall g\in\psi_z^F. \quad (16)$$

The ramp-up and down limitation of thermal generators are formulated as follows:

$$\begin{cases} P^{z,g,t+1} - P^{z,g,t} \le RU^{z,g}\cdot G^{z,g} \\ P^{z,g,t} - P^{z,g,t+1} \le RD^{z,g}\cdot G^{z,g} \end{cases}. \quad (17)$$

The minimum ON/OFF time constraints of thermal generators are formulated as follows:

$$U_{\text{on}}^{z,g,t} \ge \sum_{\tau=t-T_{\text{on}}^{z,g}}^{t} S_{\text{on}}^{z,g,t} \quad (18)$$

$$G^{z,g} - U_{\text{on}}^{z,g,t} \ge \sum_{\tau=t-T_{\text{off}}^{z,g}}^{t} D_{\text{down}}^{z,g,t} \quad (19)$$

where (18) represents minimum up times rules that require all capacity that was started up during minimum uptime interval. Minimum downtime constraint is formulated in (19).

To address system generation adequacy, the planning reserve constraint is formulated to measure the amount of generation capacity available to meet expected demand in the planning horizon. The capacity credit value varies by generation technology. For simplicity, the capacity credit value is fixed by generation technology

$$\sum_{g\in\Psi_z^G} \beta^{z,g}\cdot G^{z,g} + \sum_{s} G_{\text{ES},P}^{z,s}$$

$$\geq \max\left(D^{z,t} + \sum_{v\in\Psi_z^{\mathrm{BEV}}} P_{\mathrm{EV}}^{z,v,t}\right) \tag{20}$$

where the second term in the right-hand side represents the maximum charging power requirement for BEVs.

Spinning reserve constraints ensure that the generation fleet has enough up- and down-ramping capacity to address possible forecast errors, generation, or transmission outages. Constraint (21) defines upward spinning reserves supplied by thermal generators and energy storage systems. Constraint (22) defines downward spinning reserves supplied by thermal generators, energy storage systems, and wind/solar PV. Wind and solar can provide downward services by generation curtailment. Constraint (23) ensures that the output of thermal generators should be above downward reserves and below commit capacity minus upward reserves

$$\sum_{g\in\psi_z^F} P_{\mathrm{up}}^{z,g,t} + \sum_{z} P_{Dis,\mathrm{up}}^{z,s,t} \geq R_{\mathrm{load}}^{\mathrm{up}}\left(D^{z,t} + \sum_{v\in\psi_z^{\mathrm{BEV}}} P_{\mathrm{EV}}^{z,v,t}\right) + R_{\mathrm{RES}}^{\mathrm{up}} \sum_{g\in\psi_z^R} P^{z,g,t} \tag{21}$$

$$\sum_{g\in\psi_z^F} P_{\mathrm{down}}^{z,g,t} + \sum_{s} P_{Dis,\mathrm{down}}^{z,s,t} + \sum_{g\in\psi_z^R} P^{z,g,t} \geq R_{\mathrm{RES}}^{\mathrm{down}} \sum_{g\in\psi_z^R} P^{z,g,t} + R_{\mathrm{load}}^{\mathrm{down}}\left(D^{z,t} + \sum_{v\in\psi_z^{\mathrm{BEV}}} P_{\mathrm{EV}}^{z,v,t}\right) \tag{22}$$

$$P_{\mathrm{down}}^{z,g,t} \leq P^{z,g,t} \leq U_{\mathrm{on}}^{z,g,t} - P_{\mathrm{up}}^{z,g,t}, \forall g \in \psi_z^G. \tag{23}$$

D. CO_2 Emission Constraints

CO_2 emissions come from coal-fired power plants and gas-fired power plants for power generation and internal combustion engine vehicle (ICEVs) for powering vehicles through fuels, such as gasoline and diesel. The annual CO_2 emissions of the integrated energy system are limited by CO_2 emission cap

$$\sum_{z,t,g\in G^F} P^{z,g,t}\cdot h^g \cdot e_{emi}^f + \sum_{z,v\in\phi^{\mathrm{ICV}}} N_{z,v}\cdot \mathrm{VDT}_v \cdot fcr_v e_{emi}^f \leq \mathrm{EM}_{\mathrm{CO2}}. \tag{24}$$

E. Modeling Storage System Dynamics

The energy constraints of battery are formulated from (25) to (28). Equation (25) tracks the evolution of the stored energy level of battery based on the charge and discharge power at each time period. Constraints (26) and (27) limit the charge/discharge power capacity and energy level of battery. Constraints (28) ensures that the energy level at the initial and end of each day should be equal

$$E_{\mathrm{ES}}^{z,s,t+1} = E_{\mathrm{ES}}^{z,s,t} + P_{Ch}^{z,s,t}\cdot\eta_{\mathrm{in}}^s\cdot\Delta t - \frac{P_{Dis}^{z,s,t}}{\eta_{\mathrm{out}}^s}\cdot\Delta t \tag{25}$$

$$\begin{cases} 0 \leq P_{Ch}^{z,s,t} \leq G_{\mathrm{ES},p}^{z,s} \\ 0 \leq P_{Dis}^{z,s,t} \leq G_{\mathrm{ES},p}^{z,s} \end{cases} \tag{26}$$

$$G_{\mathrm{ES},E}^{z,s}\cdot\underline{\varepsilon_{\mathrm{ES}}} \leq E_{\mathrm{ES}}^{z,s,t} \leq G_{\mathrm{ES},E}^{z,s}\cdot\overline{\varepsilon_{\mathrm{ES}}} \tag{27}$$

$$E_{\mathrm{ES}}^{z,s,\tau\cdot 24} = E_{\mathrm{ES}}^{z,s,0}. \tag{28}$$

The balance of hydrogen flows of P2P system is achieved by (29). The outflow hydrogen of the P2P system is divided to two parts. One part is used to supply the electrical demand via fuel cell systems and rest of hydrogen is used to supply hydrogen demand of HRSs. Equation (30) and Equation (31) limit the charge and discharge power constraints of P2P system, respectively. Equation (31) defines maximum hydrogen flow limitation of pipelines. The hydrogen deliver cannot exceed the maximum capacity of HRSs. The flow rate of pipelines is assumed to be the constant value based on the parameters of pipelines. Equation (32) limits the minimum and maximum stored hydrogen level of P2P system. Constraints (33) ensures energy balance in multidays, as the maximum discharging duration may exceed 24 h

$$E_{\mathrm{ES}}^{z,s,t+1} = E_{\mathrm{ES}}^{z,s,t} + P_{Ch}^{z,s,t}\cdot\eta_{\mathrm{in}}^s\cdot\Delta t - \frac{P_{Dis}^{z,s,t}\cdot\Delta t}{\eta_{\mathrm{out}}^s} - \frac{H_{Dis}^{z,s,t}\cdot\Delta t}{\eta_{\mathrm{pipe}}^z} \tag{29}$$

$$\begin{cases} 0 \leq P_{Ch}^{z,s,t} \leq G_{\mathrm{ES},p}^{z,s} \\ 0 \leq P_{Dis}^{z,s,t} \leq G_{\mathrm{ES},p}^{z,s} \end{cases} \tag{30}$$

$$0 \leq H_{Dis}^{z,s,t} \leq \min\left(f_{fr}\left(G_{\mathrm{pipe}}^{z,r}\right), G_{\mathrm{HRS}}^z\right) \tag{31}$$

$$G_{\mathrm{ES},E}^{z,s}\cdot\underline{\varepsilon_{\mathrm{ES}}} \leq E_{\mathrm{ES}}^{z,s,t} \leq G_{\mathrm{ES},E}^{z,s}\cdot\overline{\varepsilon_{\mathrm{ES}}} \tag{32}$$

$$E_{\mathrm{ES}}^{z,s,\tau\cdot 24} = E_{\mathrm{ES}}^{z,s,0}. \tag{33}$$

The balance of hydrogen flows of HRSs is calculated by (34). The difference between the inflow from P2G systems and consumed hydrogen from FCEVs is stored in the HRSs. Equation (35) works as a constraint that limits the maximum amount of hydrogen injection into the FCEVs. Equation (36) ensures that the hydrogen stored level of HRSs is constrained within energy stored capacity. Equation (37) ensures that the planning capacity of HRS needs to exceed the daily hydrogen demand of FCEVs

$$Q_{\mathrm{HRS}}^{z,t+1} = Q_{\mathrm{HRS}}^{z,t} + \frac{H_{Dis}^{z,s,t}}{fe_{H2}}\cdot\Delta t - \sum_{v\in\Psi_z^{\mathrm{FCEV}}} \frac{Q_{\mathrm{FCEV}}^{z,v,t}}{\eta_{\mathrm{EV}}^v}\cdot\Delta t \tag{34}$$

$$0 \leq \sum_{v\in\Psi_z^{\mathrm{FCEV}}} Q_{\mathrm{FCEV}}^{z,v,t} \leq G_{\mathrm{HRS}}^z \tag{35}$$

$$\underline{\varepsilon_{\mathrm{HRS}}}\cdot G_{\mathrm{HRS}}^z \leq Q_{\mathrm{HRS}}^{z,t} \leq G_{\mathrm{HRS}}^z\cdot\overline{\varepsilon_{\mathrm{HRS}}} \tag{36}$$

$$G_{\mathrm{HRS}}^z \leq \sum_{v\in\Psi_z^{\mathrm{FCEV}}} Q_{\mathrm{FCEV}}^{z,v,t}, \forall t\in[1,24]. \tag{37}$$

The storage system can provide spinning reserve. Constraint (38) ensures that the upward reserve of energy storages should be below maximum capacity minus actual output, and the downward reserve of energy storages should be below actual output. Constraint (39) and (40) limits operation region when upward/downward reserve are provided for energy storages

$$\begin{cases} 0 \le P_{Dis,\mathrm{up}}^{z,s,t} \le G_{\mathrm{ES},p}^{z,s} - P_{Dis}^{z,s,t} \\ 0 \le P_{Ch,\mathrm{down}}^{z,s,t} \le P_{Ch}^{z,s,t} \end{cases} \quad (38)$$

$$\begin{cases} G_{\mathrm{ES},E}^{z,s} \cdot \underline{\varepsilon_{\mathrm{ES}}} \le E_{\mathrm{ES}}^{z,s,t} + \left(P_{Ch}^{z,s,t} - P_{Ch,\mathrm{down}}^{z,s,t}\right) \cdot \eta_{\mathrm{in}}^{s} \cdot \Delta t \\ G_{\mathrm{ES},E}^{z,s} \cdot \overline{\varepsilon_{\mathrm{ES}}} \ge E_{\mathrm{ES}}^{z,s,t} - \frac{\left(P_{Dis}^{z,s,t} + P_{Dis,\mathrm{up}}^{z,s,t}\right)}{\eta_{\mathrm{out}}^{s}} \cdot \Delta t \end{cases} \quad (39)$$

$$\begin{cases} E_{\mathrm{ES}}^{z,s,t} + \left(P_{Ch}^{z,s,t} - P_{Ch,\mathrm{down}}^{z,s,t}\right)\eta_{\mathrm{in}}^{s}\Delta t - \frac{H_{Dis}^{z,s,t}\Delta t}{\eta_{\mathrm{pipe}}^{z}} \le G_{\mathrm{ES},E}^{z,s}\overline{\varepsilon_{\mathrm{ES}}} \\ E_{\mathrm{ES}}^{z,s,t} - \frac{\left(P_{Dis}^{z,s,t} + P_{Dis,\mathrm{up}}^{z,s,t}\right)\Delta t}{\eta_{\mathrm{out}}^{s}} - \frac{H_{Dis}^{z,s,t}\Delta t}{\eta_{\mathrm{pipe}}^{z}} \ge G_{\mathrm{ES},E}^{z,s}\underline{\varepsilon_{\mathrm{ES}}} \end{cases}. \quad (40)$$

F. Modeling Transportation Demands and Charging Dynamics

This article investigates the technical and economic potential of BEVs and FCEVs to meet both mobility travel demands and CO_2 emission constraints. The electricity/hydrogen demand from BEVs and FCEVs are then added to the electricity grid. This article utilizes the National Household Travel Survey, including driving periods (times of departure and arrival), distance traveled, dwell time, purposes of the trip, and dwell locations, to simulate the charging flexibility of BEVs [29]. A car has two states, driving on the road and parking in the place. Suppose a car is driving and consequently not connected to the power grid. The parking locations are summarized into three categories, namely home, workplace, and public place. The probability of parking a certain type of location for a car during an average day of the year is summarized based on the survey [30], [31]. The dwell location determines the charging rates and the density of charging stations. The density of charging stations is the probability of finding a charging station in a specific type of parking location. It is assumed that the charging rate, nominal charging power of charging stations (kW), is the same at the same parking location to simplify the model.

Based on the abovementioned analyses, the available charging power of vehicles in each dwell location at each time slot is determined. However, the charging decision also depends on the state of charging (SOC) of vehicles with a battery. It is assumed that vehicles start with full SOC in each several days, as vehicle ranges can meet several days' travel demands on a full charge. Battery SOC will decrease when travel occurs and increase when charging occurs. The battery SOC must be limited in a reasonable range, such as [0.2, 1]. The two charging strategies of BEVs including the unmanaged charging strategy and the smart charging strategy are studied. In the unmanaged charging strategy, once the vehicle plugs in the charging stations, the vehicle starts to charge immediately at the charging rate of the charging station, and it stops either when its departures or when the battery SOC is full. In the smart charging strategy, BEVs can optimize their charging power and time while meeting daily energy demand. The available charging power upper of BEVs is determined by dwell location, dwell time, and SOC upon arrival, as discussed previously. Charging losses are applied to reflect more realistic operation conditions. The charging flexibility of vehicles satisfies the constraints on the power supply side and grid network congestion.

There are different driving characteristics for various vehicle categories, such as dwell time, dwell location, daily distance traveled (km/day), fuel economy (kWh/km), and many others. The vehicle trips are aggregated by vehicle category based on vehicle weights: light-duty vehicles (LDV) (0–8 500 lbs.), light-heavy duty vehicles (LHDV) (8 501–14 000 lbs.), medium-heavy duty vehicles (HDV) (14 001–33 000 lbs), and heavy-heavy duty vehicles (HHDV) (>33 000 lbs) [32].

In the unmanaged charging strategy of BEVs, the hourly charging demand of a BEV fleet is simulated based previously discussed. Then, the hourly charging demand of BEVs is exogenously added to the hourly demand of the power grid based on the total BEV fleet population

$$P_{\mathrm{EV}}^{z,v,t} = N_{z,v} \cdot \mathrm{EVD}h_{\mathrm{EV}}^{z,v,t}, v \in \psi_z^{\mathrm{BEV}}. \quad (41)$$

In the smart charging strategy of BEVs, the charging dynamic process of BEVs can be formulated as follows:

$$E_{\mathrm{EV}}^{z,v,t} = E_{\mathrm{EV}}^{z,v,t+1} + P_{\mathrm{EV}}^{z,v,t}\eta_{\mathrm{EV}}^{v}\Delta t - \mathrm{PVDT}_{\mathrm{EV}}^{z,v,t}\mathrm{VDT}_{\mathrm{EV}}^{v} fcr_v \Delta t \quad (42)$$

$$\underline{\varepsilon_{EV}} \cdot N_{z,v} \cdot Ener\mathrm{EV}_{\mathrm{EV}}^{v} \le E_{\mathrm{EV}}^{z,v,t} \le \overline{\varepsilon_{\mathrm{EV}}} \cdot N_{z,v} \cdot Ener\mathrm{EV}_{\mathrm{EV}}^{v} \quad (43)$$

$$0 \le P_{\mathrm{EV}}^{z,v,t} \le N_{z,v} \cdot \sum_{p} ProLoc_{\mathrm{EV}}^{v,p,t} \cdot \mathrm{CPEV}_{\mathrm{EV}}^{v,p} \cdot Cap\mathrm{EVSE}_{\mathrm{EV}}^{v,p} \quad (44)$$

$$\sum_{p} ProLoca_{\mathrm{EV}}^{v,p,t} = 1 - \mathrm{PVDT}_{\mathrm{EV}}^{z,v,t} \quad (45)$$

$$E_{\mathrm{EV}}^{z,v,0} = E_{\mathrm{EV}}^{z,v,\alpha\cdot 24} \quad (46)$$

where (42) represents the dynamic energy balance of BEVs. The percent of daily VDT of various vehicle categories is derived from Fig. 2. Equation (43) asserts that the cumulative charging energy must be between the upper and lower energy boundaries. Equation (44) only allows charging within the maximum aggregated charging power rate constraints and does not allow energy back to the grid. Equation (46) makes sure that a vehicle starts with full SOC every τ day.

One advantage of FCEVs is faster refueling time over BEVs. The hydrogen demands of FCEVs are supplied by HRSs, where a typical HRS today has a capacity from 100 to 1500 kg/day. HRSs are supplied by truck trailers or pipelines from central hydrogen production sources. The capacity of HRSs is planned to meet the hourly hydrogen demand of FCEVs. The average hourly hydrogen dispensing profiles of HRSs for a demonstration in California held by the National Fuel Cell Research Center [33], as shown in Fig. 3. The profiles have the average daily demand of 210 kg/day.

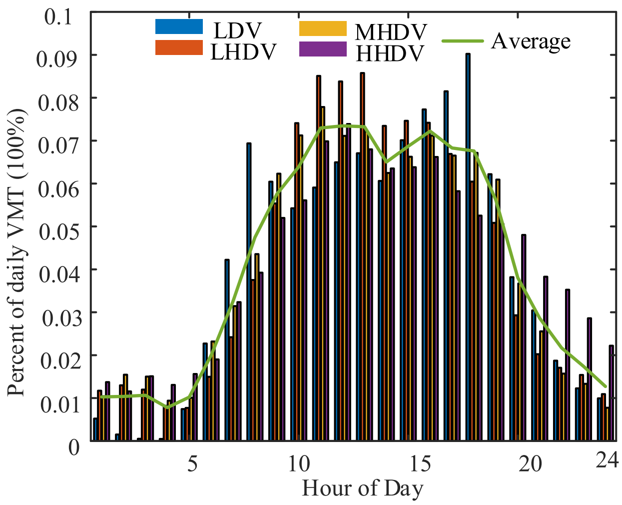

Fig. 2. Percent of daily VMT distribution by vehicle category.

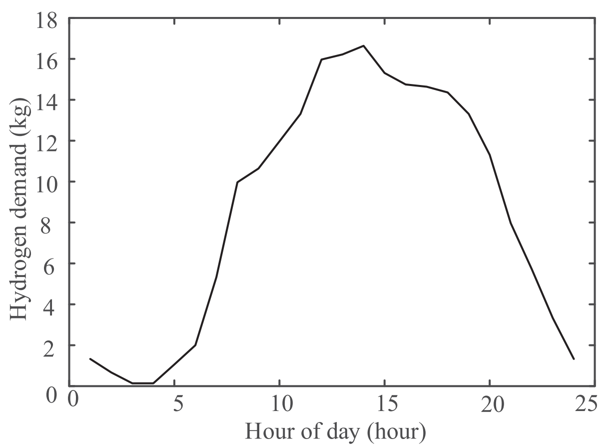

Fig. 3. Average hourly dispensing profiles for a HRS in all years. The HRS has a capacity of 360 kg/day for receiving hydrogen from a 250 kg tube trailer.

TABLE I
TECHNO-ECONOMIC ASSUMPTIONS FOR GENERATION TECHNOLOGIES

Parameters	Coal	Gas	Wind	Solar	Gas-CCS
Heat rate (kWh/Btu)	10.48	7.82	-	-	10.46
Fuel price ($/MMBTU)	2	3	0	0	0.64
Lifetime (year)	30	30	25	25	30
Max. output (%)	100	100	100	100	100
Min. output (%)	0	0	0	0	0
Capital cost ($/kW)	3711/ 3346/ 3346	906/ 782/ 782	1445/ 1118/ 939	1325 /782/ 673	6200/ 5085/ 5085
Fixed O&M (% of Capital cost)	1	1	2.5	2	1.5
Variable O&M cost ($/MWh)	5	3	0	0	2
Start-up cost ($/MW)	147	88	0	0	-
Min. up time (h)	24	1	-	-	-
Min. down time (h)	48	1	-	-	-
Ramping limit (%/hr.)	35	50	-	-	50
Min. load level (%)	50	0	0	0	0
Capacity credit (%)	100	100	20	20	100

Notes: There are three values in a single cell for capital cost, in which they refer to cost scenario in 2020, 2035, and 2050.

IV. DATA AND SCENARIOS

A. Power System Data

The model is applied to the U.S. State of Texas served by the Electric Reliability Council of Texas (ERCOT) that manages the flow of electric power to Texas customers, covering approximately 90% of the state's electricity load. ERCOT is largely electrically isolated from the rest of North America and is modeled as an isolated grid [34].

Geographically, there are eight load zones that are consistent with the ERCOT's eight weather zones, namely, South, South Central, Coast, East, West, Far West, North, and North Central. The electricity transmission network is adapted from the existing U.S. test systems [35]. Each transmission line has a nominal capacity limitation. In the planning process, IPTS can expand its capacity. Transmission losses with 1% per 100 miles are considered. The long-distance inter-regional transmission lines with 345 kV are applied for each load zone. The capital cost of transmission lines is assumed to be $2,333/MW-mile for 345 kV [36].

Regarding to the generation capacity and renewable generation profiles, in 2018, the total capacity was 86.6 GW, and total generation was 376 000 GWh. Natural gas- and coal-fired generators are assumed dispatchable and their information are obtained from Form EIA-860 and EIA-923 data [37]. The generation profiles of nuclear, biomass, hydropower, solar, and wind units are fixed based on historical hourly generation profiles. The historical hourly power profiles for operational wind, 30.9 GW of hypothetical wind, 5.9 GW of hypothetical utility-scale solar for the period of 1980 through 2019 are obtained from the ERCOT [38]. The potential wind and solar capacity are scaled to 300 GW and 50 GW to realize a zero-emission scenario. The hourly historical load demand is obtained from ERCOT. Moreover, the gas-fired power plant with carbon capture and storage (CCS) can be built in future. Table I summarizes technical parameters and cost assumptions of power generation plants.

Regarding to the energy storage technologies, this article proposes two energy storage technology option: Li-ion-based (short-term energy storage) and hydrogen-based (long-term energy storage) storage systems. Fuel cells have the potential to replace the internal combustion engine in vehicles and to provide power in stationary and portable power applications because they are energy efficient, clean, and fuel flexible [39], [40]. Fuel cell systems are selected to generate electricity using hydrogen, and Polymer Electrolyte Membrane electrolyzers are selected to produce hydrogen. Hydrogen delivery transforms hydrogen from central production to the point of use in fuel cell systems or HRSs. Typical hydrogen pipeline network with different diameter are designed in this article [1] (see Table II). The distance from P2G system to HRSs is assumed to be 100 km in each zone. The capital cost estimates of hydrogen delivery are obtained from the Hydrogen Geologic Storage Model [25].

TABLE II
TECHNO-ECONOMIC ASSUMPTIONS FOR PIPELINES

Technology type	Maximum flow rate (ton/hour)	Capital Cost ($k/km)	Assumed losses (%/km)
H_2 pipeline – 46 cm	26	870	0.005
H_2 pipeline – 61 cm	108	1260	0.005
H_2 pipeline – 91 cm	378	2020	0.005
H_2 pipeline – 122 cm	792	2790	0.005

TABLE III
TECHNO-ECONOMIC ASSUMPTIONS FOR ENERGY STORAGE TECHNOLOGIES

Technology	Round-trip efficiency	Lifetimes (yr)	Fixed O&M (% of CAPEX)	Power cost ($/kW)	Energy cost ($/kWh)
Li-ion	90%	13	1.5	260/137/110	299/157/126
Hydrogen	50% /60%/70%	20	1.5	2000 / 1350/630	5.5/3.7/1.8

TABLE IV
VEHICLE PARAMETERS

Vehicle Category	Vehicle Model	Capital Cost (10^3\$)	O&M Cost (\$/vehicle-yr)	Fuel Economy
LDV	ICEV	20/ 16/ 12	5%	0.025
	BEV	35/ 30/ 25	5%	0.198
	FCEV	58/ 43/ 27	5%	0.0104
LHDV	ICEV	39/ 31/ 23.6	5%	0.037
	BEV	51/ 43.9/ 36.7	5%	0.338
	FCEV	75/ 55/ 35	5%	0.0208
MHDV	ICEV	62/ 50 /37.5	10%	0.062
	BEV	85/ 73/ 61	10%	0.627
	FCEV	150/ 110/ 70	10%	0.0278
HHDV	ICEV	124/ 100/ 75	10%	0.067
	BEV	200/ 172/ 144	10%	1.289
	FCEV	268/ 204/ 140	10%	0.0568

Note: Unit of fuel economy of vehicle is [gallon gasoline/km] for ICEV, [kWh/100 km] for BEV, and [kg H_2/km] for FCEV.
There are three values in a single cell for capital cost, in which they refer to 2020, 2035, and 2050.

TABLE V
VEHICLE PARAMETERS

Vehicle Category	VMT (km)	EMFAC 2017	Lifetime (year)	Range (km)
LDV	72	34-39	15	560
LHDV	115	-	10	480
MHDV	118	17-170	10	480
HHDV	297	16-256	10	800

Notes: EMFAC: Emissions Factor model that provides tools and data to generate the official emissions inventories of mobile sources in California.

TABLE VI
HYDROGEN REFUELING STATION COSTS

Type	Storage level (kg/day)	Cost (million)	Cost(\$$10^3$/kg-day)
H_2 Refueling station	1000	1.8	1.8

Notes: HRS and EV charging infrastructure are assumed to have an economic lifetime of 30 years and their OPEX is assumed to be 5% of the CAPEX.

TABLE VII
ELECTRICITY VEHICLE CHARGING INFRASTRUCTURE IN US

Charging level	Voltage	Typical power	Per-charger cost/$	Location
Level 1	120V AC	1.4 kW AC	596	home
Level 2	208 - 240 V AC	6.6 kW AC	2,793	workplace
Level 3	400-1000 V DC	50 kW DC 120 kW DC	28,400 140,000	Public place

Corresponding parameters of considered storage technologies are shown in Table III [41], [42].

B. Transportation System Data

The vehicle trips are aggregated by vehicles category: LDV, LHDV, MHDV, and HHDV. The national vehicle stock by fuel type is obtained from the Bureau of Transportation Statistics [43]. The number of vehicles by load zone is estimated based on the population. The vehicle population ratio by vehicle category is used to estimate vehicle population by vehicle category in Texas. The vehicle number in Texas is regarded as the planning upper limitation for ICEVs, BEVs, and FCEVs.

Vehicle parameters such as purchase costs, fixed O&M cost, and fuel economy, are shown in Table IV [44]. Retail prices of commercial truck are obtained from the commercial truck trade website [45]. The retail price of BEVs and FCEVs are obtained from the MARKAL model dataset [46] and a wide range of credible sources. The fuel economy of vehicles is obtained from the U.S. Department of Energy [47]. The maximum and minimum fuel economy values are applied to lower and upper values for the sensitivity analyses on BEVs and FCEVs. The battery capacity/fuel tank capacity of vehicles is determined by their range and fuel economy (see Table V). A 100-mile range is approximately equivalent to a hydrogen tank capacity of 1.6 kg H_2 for LDVs, 4 kg H_2 for LHDVs, 6 kg H_2 for MHDVs, 6.9 kg H_2 for HHDVs. The average daily VMT for each vehicle category is compared to existing literature estimates (see Table V). It is assumed that the VMT of BEVs and FCEVs is the same as the ICEVs.

After hydrogen is transformed from a central production plant to the city, additional hydrogen refueling stations need to be constructed for the wide-spread adoption of FCEVs. It is assumed that all refueling stations are centered in a single point. HRSs receive compressed hydrogen from a centralized, already operational production facility. Cost data for HRS and hydrogen transmission are obtained from the IEA (2019) [41], [48]–[49] (see Table VI).

Table VII summarizes basic information regarding different charging piles [50]. California survey shows that 44% of electric vehicle drivers use charging level 1, 35% of electric vehicle drivers use charging level 2, and 11% of electric vehicle drivers use charging level 3 [51]. This utilization ratio of charging piles is used to estimate the needs of charging infrastructures of LDVs and density of charging stations in a certain type of location. For other vehicle categories, they highly rely on public charging piles with charging level 3, as they have a higher energy demand than LDVs. It is assumed that the ratio between charging piles with charging level 3 and the BEVs of non-LDVs is 0.26:1 to allow them to charge vehicles during dwell times.

TABLE VIII
SCENARIO DESCRIPTIONS

Scenario	Carbon reduction rate	Cost assumptions
Business as usual (BAU)	No carbon cap (0%)	Moderate cost scenario
Combined-no-P2G	100% - 0%	
Combined-with-P2G		
Separately-no-P2G		
Separately-with-P2G		

Texas Travel Survey Program dataset is selected, as the Texas dataset has vehicle samples for vehicle types with detailed trip data, including a driving period (times of departure and arrival), distance traveled, dwell time, the purpose of the trip, and dwell locations [52].

C. Scenarios

To investigate the optimal IPTS capacity, transmission, and vehicle population mix as determined in the proposed model. A set of scenarios are conducted, as shown in Table VIII. The combined scenario decarbonizes integrated power and transportation sectors, where the total CO_2 emissions of power and transportation sectors are constrained by the single CO_2 emission cap. However, in the separately planning scenarios, CO_2 emissions of power and transportation sectors are separately constrained by CO_2 emission caps. The combined-with-P2G and separately-with-P2G are conducted to compare the different decarbonization trajectories of IPTS. CO_2 emission caps are designed to linearly reduce from 100% (100% renewable electricity) to 0% (no carbon cap) at an interval of 10%. Business as usual (BAU) scenario without carbon cap constraint shows current operating characteristics of IPTS. Moreover, the comparison with the combined-no-P2G and combined-with-P2G scenarios highlights the impacts of P2G in decarbonizing IPTS by integrating power and transportation system through using excess RES generation. To make smart charging strategy more realistic, it is assumed that the participation rate of vehicles to participate in smart charging program is 50%. All technology costs and parameter estimates are exogenous to keep the simplicity of the calculation. The mathematical model and data processing are implemented and simulated using MATLAB, YALMIP, and GUROBI.

V. CASE STUDY

A. Comparison of Carbon Intensity and Costs Between Coordinated and Separated Planning Scenarios

Fig. 4 shows the trajectories of CO_2 emission intensity in IPTS in different carbon caps. Under the combined-with-P2G scenario, with a strict CO_2 emission cap, the power sector begins to decarbonize first, and the CO_2 emission intensity of the transportation system only begins to decline slightly around the 30% CO_2 emission cap scenario. When the CO_2 emission cap is larger than 40%, the CO_2 emission intensity of the transportation system decreases rapidly from 260 gCO_2/km in the 40% carbon cap to 105 gCO_2/km in 70% carbon cap. Meanwhile, the CO_2 emission intensity of the power system is 85 gCO_2/kWh in the 70% carbon cap, an 83% reduction compared with the BAU scenario. Conversely, under the separately-with-P2G scenario, the CO_2 emission intensity of the power and transportation system will decrease proportionally at the same time with strict CO_2 emission constraints. This is because zero-emission vehicles highly rely on electricity or hydrogen produced by P2G units, increasing corresponding CO_2 emissions from the power systems. This decarbonization sequence, advancing from the power sector to the transportation sector over time, is consistent with current policies and the notion that transportation exhibits strong carbon lock-in.

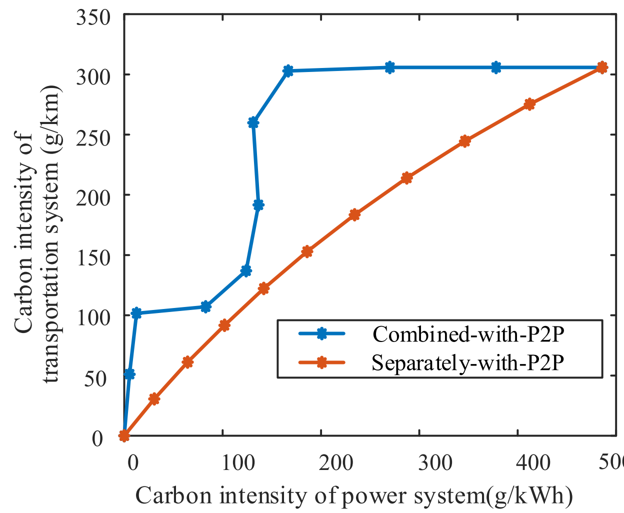

Fig. 4. Carbon intensity of the power and transportation systems under the combined-with-P2G and separately-with-P2G scenarios. The CO_2 emission intensity of the power system is the ratio of CO_2 emissions from electricity generations (g CO_2/kWh). The CO_2 emission intensity of the transportation system is the ratio of CO_2 emissions when operating vehicles (g CO_2/km), in which cover tank-to-wheel stage.

Fig. 5 illustrates the breakdown of annual IPTS costs under the combined-with-P2G and separately-with-P2G scenarios with different carbon caps. The annual economic value of the existing infrastructure of power and road transportation systems is \$17.38 billion and \$55.82 billion, respectively. The power system infrastructure (power plants and transmission grid) represents 45% of the total CO_2 emissions of IPTS, but less than 23.75% of the total estimated economic value of the existing infrastructure. On the contrary, the road transportation system (different types of vehicles) with high capital costs and short lifetimes, represents 76.25% of the total estimated economic value of existing infrastructures and 55% of total CO_2 emissions of IPTS. Moreover, if incorporating operating costs (fuel cost, fixed O&M costs, *et al.*) in IPTS, the annual total costs of the road transportation system represent 86% of the total costs of IPTS. This analysis highlights the disproportionality of CO_2 emissions per unit economic value and is consistent with the findings of decarbonization sequence in Fig. 4.

Currently, replacing the over 20 million ICEVs on the road and almost 64.5% coal and gas generation in Texas will be a tough challenge. The BAU scenario without carbon cap and 100% renewable electricity scenario result in annual total IPTS costs

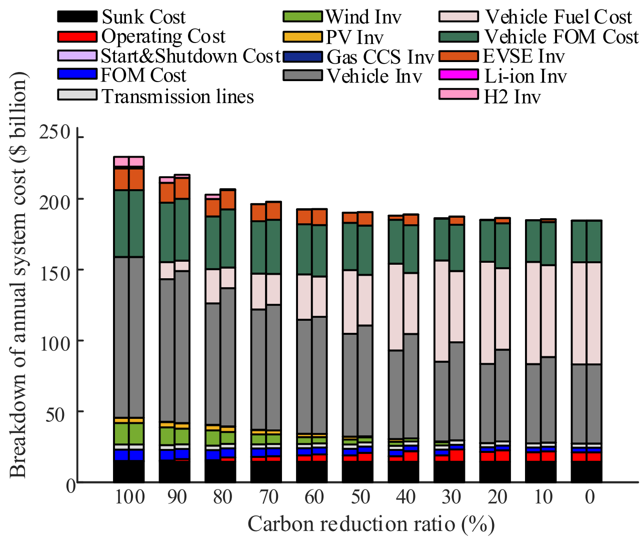

Fig. 5. Breakdown of the annual IPTS cost under the combined-with-P2G scenario (left) and separately-with-P2G scenario (right). Sunk cost summarizes the annual capital cost of all types of generation technologies. Operation cost summarizes the fuel cost and variable costs of electricity generation. Startup cost includes startup cost of thermal generators. FOM cost includes fixed O&M costs of all type pf generation technologies. Transmission lines summarizes the annual capital cost of transmission line networks. Wind INV summarizes new wind investment costs. Solar INV summarizes new solar PV investment costs. Gas-CCS is new gas-CCS investment costs. Vehicle INV summarizes the annual capital cost of all types of vehicles. Vehicle Fuel includes gasoline fuel costs of ICEV. EVSE INV includes investment costs of HRS and charging piles. Li-ion INV is investment costs of BESS. H2 INV is investment coat of hydrogen P2G systems.

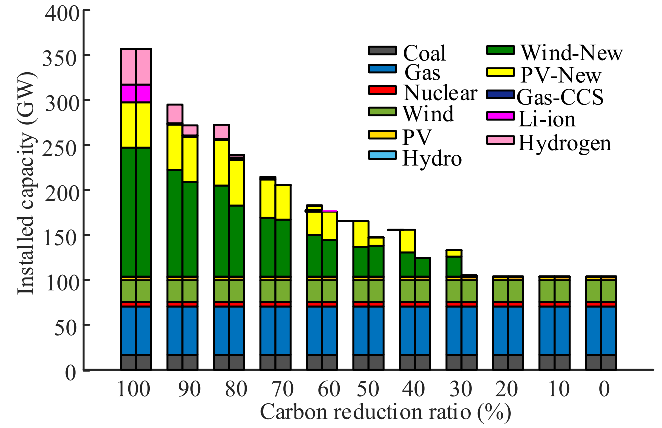

Fig. 6. Installed capacity under the combined-with-P2G scenario (left) and separately-with-P2G scenario (right).

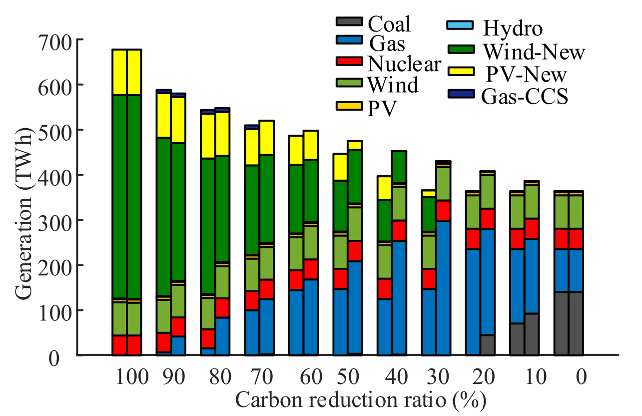

Fig. 7. Generation mixes under the combined-with-P2G scenario (left) and separately-with-P2G scenario (right). There is no item of P2G and BESS generation because the generation of P2G and BESS comes from the power grid produced by excess renewable generation.

of approximately $184.6 billion and $229.6 billion, respectively. The increase in system costs mainly results from the purchase costs of BEVs and FCEVs, corresponding charging/refueling infrastructure costs, and investment costs of renewables and energy storage. Moreover, adopting the coplanning method under the combined-with-P2G scenario can save annual total cost ranging from 0 to 2% under various CO_2 emission caps. The cost benefits of the proposed coordinated planning model mainly occur in high-proportion emission reduction scenarios. This indicates a negligible cost-saving benefits compared with the separately-with-P2G scenario. This is because the proposed model does not consider the replacement costs of replacing existing ICEVs and consumers' willingness to purchase BEVs or FCEVs that are affected by many factors, such as purchase cost, vehicle range, EVSE, financial incentives, individual environmental awareness. The analysis reveals that union climate policies and actions in IPTS may be cost-effective and produce an optimal trajectory for the IPTS.

B. Generation and Capacity Mix of Power System

Under the BAU scenario, ERCOT has over 103 GW of installed capacity, composed of 52.2% natural gas, 23.1% wind, 15.5% coal, 5.0% nuclear, and other sources. Fig. 6 shows the optimal installed capacity in various carbon caps. Gas-CCS will be installed to provide IPTS quick ramping up/down reserve at low CO_2 emissions when the CO_2 emission reduction is between 70% and 90%. The share of Gas-CCS capacity in total capacity is less than 1% across scenarios due to its higher capital costs. The Gas-CCS will not work during a 100% renewable electricity scenario. The existing coal and natural gas generation capacity will remain to meet the planning reserve constraint that maintains system generation adequacy requirement. Without any added RES generation capacity, IPTS of Texas could achieve 20% CO_2 emissions reductions through fuel switching. With the increasing CO_2 emission reduction requirements, replacing coal generation with gas generation is adopted first to meet CO_2 emission reduction targets (see Fig. 7). In Fig. 7, under the combined-with-P2G scenario, coal generation will decrease dramatically from 140 TWh under without carbon cap constraints to approximately 1.0 TWh under the 20% carbon cap. While gas generation still plays an important role before the 80% carbon reduction ratio. Especially, the share of gas generation in total generation accounts for over 69% under the 30% carbon cap under the separately-with-P2G scenario. It is consistent with the near-term trends in the US, in which natural gas generation exceeded coal generation in 2015.

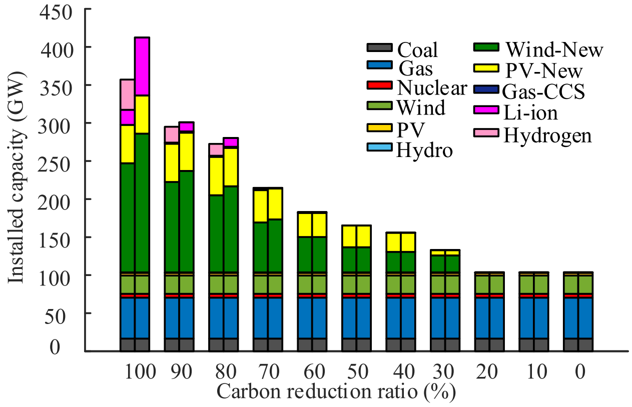

Fig. 8. Installed capacity under the combined-with-P2G scenario (left) and combined-no-P2G scenario (right).

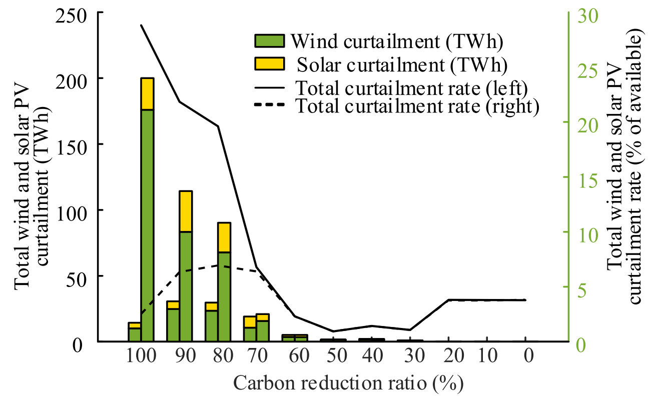

Fig. 9. Curtailment of wind and solar PV (left vertical axis) and curtailment rate of wind and solar PV (right vertical axis) under the combined-with-P2G (left) and combined-no-P2G scenario (right).

The main drivers for generation capacity, energy storage, and transmission grid are increasing carbon caps and energy demand from mobility. The IPTS prefers to installing wind plants to replace coal and gas generation due to its lower levelized cost of energy (LCOE) relative to solar PV. Under the combined-with-P2G scenario, wind capacity increases from 23.9 GW without carbon cap to 143.5 GW with zero-emission constraint, accounting for approximately 40.2% of the total capacity. Solar PV installed capacity reaches its peak (50 GW) earlier under 80% carbon reduction requirement. The share of wind and solar PV power in total generation mixes increases from 22.4% without carbon cap to 93.3% in 100% carbon reduction requirements. There is a significant gap between the current 30.9 GW of hypothetical wind and 5.9 GW of hypothetical utility-scale solar and optimal capacity mixes in the Texas.

Similar results are found in the Texas case study from Arbabzadeh *et al.* [53], in which adding 60 GW of renewable to Texas could achieve 57% emission reductions in 2012. In our case study, adding a total of 78 GW wind and solar PV to Texas could achieve 60% CO_2 emission reductions in 2018 under the combined-with-P2G scenario. This is because the IPTS needs to meet not only electricity demand, but also mobility energy demand from BEV and FCEV.

C. Impact of Hydrogen P2G System on Renewable Curtailment and Capacity Mix

To investigate the impact of hydrogen P2G systems on renewable curtailment and optimal capacity mix, two scenarios, the combined-with-P2G, and combined-no-P2G scenarios are compared. The capacity mixes with and without access to hydrogen P2G systems are compared in Fig. 8. Without any access to energy storage, IPTS of Texas could achieve 70% CO_2 emission reductions, through the large-scale deployment of RESs, Gas-CCS, and BEVs.

The integration of P2G system produces significant results compared with the scenario without P2G system. First, the curtailment of RES generation reduces significantly. For instance, for the combined-no-P2G scenario, despite the significant deployment of short-term storage capacity (Li-ion BESS of 76 GW/760 GWh, or $\sim$ 18.5% of total installed capacity) in 100% carbon cap, the curtailment rate of total wind and solar PV generation would be approximately 28.8% as wind and solar PV are largely deployment (see Fig. 9). On the contrary, adding hydrogen P2G systems (40 GW/4377 GWh) and Li-ion BESS (20 GW/39 GWh) declines RES curtailment by approximately 93% under the combined-with-P2G scenario, compared with the combined-no-P2G scenario (see Fig. 9). The results indicate that increasing the penetration rate of RESs enables hydrogen P2G systems more cost-effective. Second, hydrogen P2G enables coupling power and transportation systems. This is because excess RES generation can be used to produce hydrogen to meet FCEV's fuel demand or meet the electricity demand of the power system. Additionally, deployment of P2G system under the combined-with-P2G scenario could reduce RES capacity requirement by 13.4% in 100% renewable electricity system relative to the combined-no-P2G scenario.

D. Hourly Dispatch of IPTS

The hourly power balances for 12 consecutive days under the 0% carbon cap, zero-emission scenario with and without P2G system are compared in Fig. 10. The peak electricity demand is 63.2 GW under the BAU scenario. Gas-fired generation is widely used to meet peak loads under the BAU scenario, as shown in Fig. 10(a). Large-scale deployment of RES generation capacity, BEV, and FCEVs results in significantly different operating characteristics, such as load balancing, peak demand, and flexibility requirements. The power demand from the growing BEV and FCEV fleet results in a significant increase in peak demand. In Fig. 10(b), additionally, the maximum charging demand from BEV is 51 GW. When added BEV-HHDV under the combined-no-P2G scenario, additionally maximum peak demand from BEV increases to be 60 GW, as shown in Fig. 10(c).

In this article, participation rate of vehicles to participate in smart charging program is assumed to be 50%. Charging demand of controllable BEVs is optimized to shift to OFF-peak hours to charge with surplus wind generation, because total net peak load determines the minimum planning for dispatchable generation

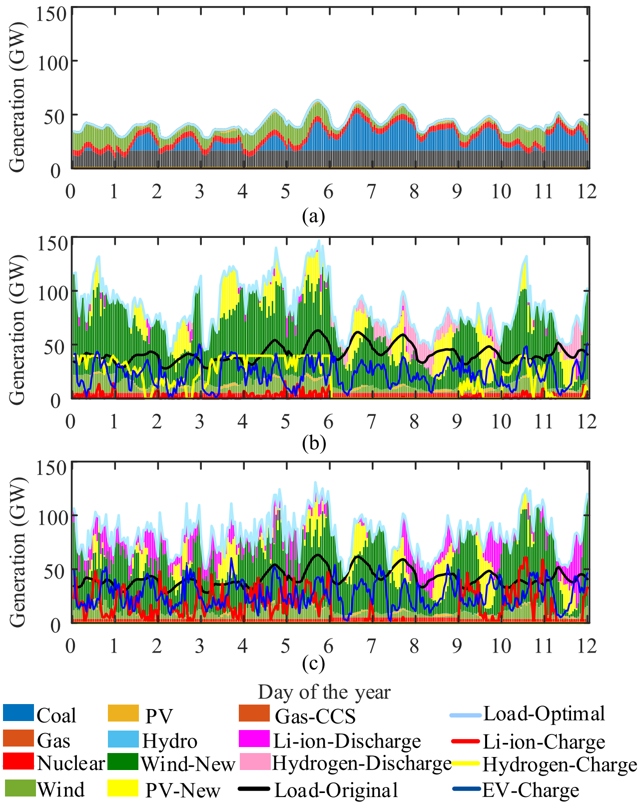

Fig. 10. In total, 12 consecutive days of simulated hours. (a) 0% CO_2 cap; (b) 100% CO_2 cap with P2G; (c) 100% CO_2 cap without P2G scenario.

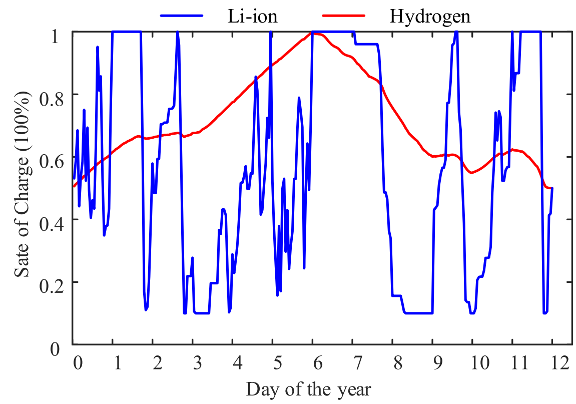

Fig. 11. Normalized SOC of energy storage systems under the combined-with-P2G scenario.

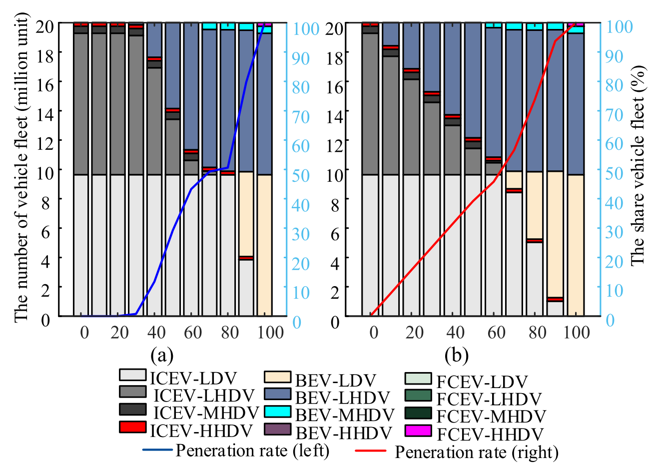

Fig. 12. Vehicle population mix (left vertical axis) and penetration rate of total BEV and FCEV fleet (right vertical axis); (a) combined-with-P2G scenario; (b) separately-with-P2G scenario.

capacity and hourly spinning reserve capacity requirements. In the proposed model, the BEVs charging rates are limited by charging flexibility, including dwell time and locations, and charging infrastructure capabilities and availability. The results reveal that as the power sector incorporates more charging demand from BEVs, charging infrastructures will become more important to allow BEVs to respond quickly from electricity price signal and regulation signal so that coordinated charging strategy can be aligned with a high penetration level of renewable energy sources.

Based on hourly optimized dispatch results of IPTS, the SOC curve of BESS and hydrogen P2G system are illustrated in Fig. 11. Li-ion-based BESS with short discharging hours has more intraday fluctuations than the corresponding SOC curve of P2G system, as P2G system has more longer discharging hour of 108 h than BESS discharging hour of approximately 2 h. Hydrogen produced by P2G units using surplus renewables power can be transformed for transportation fuels of FCEV-HHDVs, the residual hydrogen is used to discharge to satisfy daily power imbalances in the ninth and twelfth days, in which the days have lower RES generation.

E. Transportation System

BEVs and FCEVs with no operating emissions and, thus, offer the significant potential to reduce CO_2 emissions from road mobility. The vehicle population mix and penetration rate of BEV and FCEV fleet in different CO_2 emission caps under the combined-with-P2G and separately-with-P2G scenarios is shown in Fig. 12. The transportation sector's vehicle population mix is not likely to undergo major change without CO_2 emission cap constraints if there is no action in decreasing the purchase costs of alternative fuel vehicles. For instance, Fig. 12(a) reveals that BEV-LHDV is deployed first to replace ICEV-LHDV to reduce CO_2 emissions of the road transportation system when the carbon cap is larger than 20%. When the carbon cap is 70%, almost all ICEV-LHDV is replaced by BEV, reaching 9.37 million units. Meanwhile, almost all ICEV-MHDV is replaced by BEV, reaching 0.46 million units. When the carbon cap is 90%, BEV-LDV begins to be deployed to replace ICEV-LDV. ICEV-LDV of 5.78 million is replaced by BEV under the 90% carbon cap constraints. ICEV-HHDV is the hardest vehicle type to be decarbonized during all types of vehicles.

Additionally, under the combined-with-P2G scenario, the penetration rate of BEV and FCEV fleet will increase significantly from 11.8% under the 40% carbon cap to 100% under 100% carbon cap. However, the penetration rate of BEV and FCEV begins to increase almost proportionally from 7.8% in

10% carbon cap. The analysis indicate coordinated planning method for IPTS will switch the merit order between the power and transportation system.

The heavy-duty long-haul drive segment, including trucks and buses, offer strong prospects for hydrogen FCEVs, as it requires long-range and high fuel demands. Under the combined-with-P2G scenario, the ICEV-HHDV will be replaced by FCEV-HHDV during 100% renewable electricity, indicating FCEV-HHDV tend to be more competitive against BEV-HHDV. The number of FCEV-HHDV is 0.24 million units, leading to daily hydrogen demand of 3.6 million kg (P2G system of 1 MW with efficiency of 51.2 kWh/kg H2 can produce maximum 436 kg hydrogen per day). To corporate with the use of FCEV, the roll-out of P2G system, hydrogen deliver networks, and HRSs are key requirements for systems. For instance, there are equivalent 1 800 HRSs, each of them has a capacity of 1 000 kg H2/day. The total investment cost to build these 1 800 HRSs will be USD 3.24 billion. To meet the needs of growing FCEVs, policymakers should pay attention to refueling infrastructures at the right time, as hydrogen fueling infrastructures are less common.

VI. Conclusion

As the large-scale deployment of BEVs and FCEVs in road transportation system, the power system, and road transportation system are increasing interweaving with each other. A coordinated long-term planning model for the integrated power and road transportation system is proposed to investigate the cost-effective decarbonization pathway incorporating hydrogen P2G systems. The model is based on ERCOT of Texas and considers energy demand of road transportation system involving different vehicle types and fuel types.

The IPTS of Texas shows different decarbonization trajectory toward zero-emissions scenario compared with noncoordinated planning model of IPTS. The optimal decarbonization pathway includes two main stages: IPTS prefers to decarbonizing the power sector first through fuel switching, deployment of RESs and energy storage systems. When the power system reaches ultralow carbon intensity, the IPTS then focus on the road transportation system decarbonization through replacement ICEV by BEV and FCEV fleet.

For the power system, wind capacity contributes a major source for generation mix resulting from its lower LCOE and rich wind generation potential in Texas relative to solar PV. The results show P2G system has a significant role in decarbonizing IPTS through greater use of excess RESs. Without P2G system, massive RES deployment is requirement due to higher RES curtailments. In Texas, P2G system deployment yields 93% RES curtailment reduction compared with no-P2G case under 100% renewable electricity. Additionally, the results show the role of P2G system in integrating power and road transportation system. At very high-RES penetrations, P2G system can produce hydrogen by use of surplus RES generation to meet hydrogen demand of FCEVs and to meet multiday electricity supply imbalances.

For the road transportation sector, conventional heavy-duty long-haul vehicles, like trucks and buses, are the hardest vehicle type to be shifted to zero-emission vehicles (BEVs and FCEVs). Private transportation, like light-duty vehicles, are transmitted to BEVs. In segments such as heavy-duty, long-haul trucking, new technology breakthroughs and cost reduction for zero-emission vehicles will be required to sufficiently decrease CO_2 emissions. Optimized charging demand profiles of BEVs are crucial to grid operation with a high penetration level of renewable energy sources.

The method to model decarbonization strategies in several energy system sectors in this article demonstrates the benefits from coordination between electricity and transport sectors in regional scale. While the coordinated planning of decarbonization strategies in different sectors of the energy system can increase cost- and resource efficiency, it is important to have functioning communication and collaboration between various stakeholders. Therefore, to promote the climate movement, it is important to call on the government to have greater ambitions to establish a cross departmental and cross-party low-carbon planning and implementation department. China established the "Carbon Peak and Carbon Neutrality Work Leading Group" in 2021 to guide and supervise localities and key areas, industries, and enterprises to scientifically set goals and plans to achieve carbon peak in 2030 and carbon neutrality in 2060. The US has the "House Select Committee on the Climate Crisis" that is charged with coordinating and advancing policies, strategies, and innovations to achieve substantial and permanent reductions in pollution and other activities that contribute to the climate crisis. Thus, it is important to have a functioning communication and collaboration between various stakeholders.

References

[1] Department for Business Energy and Industrial Strategy, "Hydrogen supply chain: evidence base," 2018. [Online]. Available: https://www.gov.uk/government/publications/hydrogen-supply-chain-evidence-base

[2] J. Wang et al.*et al.*, "Exploring the trade-offs between electric heating policy and carbon mitigation in China.," *Nat. Commun.*, vol. 11:6054, 2020, doi: 10.1038/s41467-020-19854-y.

[3] P. Albertus, J. S. Manser, and S. Litzelman, "Long-Duration electricity storage applications, economics, and technologies," *Joule*, vol. 4, no. 1, pp. 21–32, 2020.

[4] O. J. Guerra, J. Zhang, J. Eichman, P. Denholm, J. Kurtz, and B.-M. Hodge, "The value of seasonal energy storage technologies for the integration of wind and solar power," *Energy Environ. Sci.*, vol. 13, no. 7, pp. 1909–1922, 2020.

[5] A. Wanitschke and S. Hoffmann, "Are battery electric vehicles the future? An uncertainty comparison with hydrogen and combustion engines," *Environ. Innov. Soc. Transitions*, vol. 35, pp. 509–523, 2020.

[6] B. Li *et al.*, "Modeling the impact of EVs in the Chinese power system: Pathways for implementing emissions reduction commitments in the power and transportation sectors," *Energy Policy*, vol. 149, 2021, Art. no. 111962.

[7] D. Zhao, M. Zhou, J. Wang, et al.*et al.* "Dispatching fuel-cell hybrid electric vehicles toward transportation and energy systems", to be published, *CSEE Journal of Power and Energy Systems*, 2021. Online available: https://www.researchgate.net/publication/350425595_Dispatching_Fuel-Cell_Hybrid_Electric_Vehicles_toward_Transportation_and_Energy_Systems_Integration

[8] J. K. Szinai, C. J. R. Sheppard, N. Abhyankar, and A. R. Gopal, "Reduced grid operating costs and renewable energy curtailment with electric vehicle charge management," *Energy Policy*, vol. 136, 2020, Art. no. 111051.

[9] H. Zhang, Z. Hu, Z. Xu, and Y. Song, "Evaluation of achievable Vehicle-to-Grid capacity using aggregate PEV model," *IEEE Trans. Power Syst.*, vol. 32, no. 1, pp. 784–794, Jan. 2017.

[10] B. Li *et al.*, "Integration of battery electric vehicles in a regional hydro–wind–thermal power system," *Energy Rep.*, vol. 6, pp. 1199–1205, 2020.
[11] M. Zhou, Z. Wu, J. Wang, and G. Li, "Forming dispatchable region of electric vehicle aggregation in microgrid bidding," *IEEE Trans. Ind. Inform.*, vol. 17, no. 7, pp. 4755–4765, Jul. 2021.
[12] V. Heinisch, L. Göransson, R. Erlandsson, H. Hodel, F. Johnsson, and M. Odenberger, "Smart electric vehicle charging strategies for sectoral coupling in a city energy system," *Appl. Energy*, vol. 288, 2021, Art. no. 116640.
[13] L. Jian, Z. Yongqiang, and K. Hyoungmi, "The potential and economics of EV smart charging: A case study in Shanghai," *Energy Policy*, vol. 119, pp. 206–214, 2018.
[14] X. Chen, J. Lv, M. B. McElroy, X. Han, C. P. Nielsen, and J. Wen, "Power system capacity expansion under higher penetration of renewables considering flexibility constraints and low carbon policies," *IEEE Trans. Power Syst.*, vol. 33, no. 6, pp. 6240–6253, Nov. 2018.
[15] T. Zhang, J. Wang, H. Zhong, G. Li, M. Zhou, and D. Zhao, "Soft open point planning in renewable-dominated distribution grids with building thermal storage," *CSEE J. Power Energy Syst.* (early access), pp. 1–9, 2020, doi: 10.17775/CSEEJPES.2020.03660.
[16] C. F. Heuberger, P. K. Bains, and N. Mac Dowell, "The EV-olution of the power system: A spatio-temporal optimisation model to investigate the impact of electric vehicle deployment," *Appl. Energy*, vol. 257, 2020, Art. no. 113715.
[17] M. T. Brozynski and B. D. Leibowicz, "Decarbonizing power and transportation at the urban scale: An analysis of the Austin, Texas community climate plan," *Sustain. Cities Soc.*, vol. 43, pp. 41–54, 2018.
[18] P. Colbertaldo, G. Guandalini, and S. Campanari, "Modelling the integrated power and transport energy system: The role of power-to-gas and hydrogen in long-term scenarios for Italy," *Energy*, vol. 154, pp. 592–601, 2018.
[19] International Renewable Energy Agency, "Electricity storage and renewables: Costs and markets to 2030," 2017. [Online]. Available: https://www.irena.org/publications/2017/oct/electricity-storage-and-renewables-costs-and-markets
[20] C. Wulf, J. Linssen, and P. Zapp, *Power-to-Gas—Concepts, Demonstration, and Prospects*. San Francisco, CA, USA: Academic, 2018.
[21] J. E. and F. Flores-Espino, "California Power-to-Gas and Power-to-Hydrogen Near-Term Business Case Evaluation," *Natl. Renew. Energy Lab.*, 2016, [Online]. Available: https://www.nrel.gov/docs/fy17osti/67384.pdf
[22] P. Colbertaldo, S. B. Agustin, S. Campanari, and J. Brouwer, "Impact of hydrogen energy storage on California electric power system: Towards 100% renewable electricity," *Int. J. Hydrogen Energy*, vol. 44, no. 19, pp. 9558–9576, 2019.
[23] B. Widera, "Renewable hydrogen implementations for combined energy storage, transportation and stationary applications," *Thermal Sci. Eng. Prog.*, vol. 16, 2020, Art. no. 100460.
[24] S. Kuczynski, M. Łaciak, A. Olijnyk, A. Szurlej, and T. Włodek, "Thermodynamic and technical issues of hydrogen and methane-hydrogen mixtures pipeline transmission," *Energies*, vol. 12, no. 3, p. 569, 2019.
[25] A. S. Lord, P. H. Kobos, and D. J. Borns, "Geologic storage of hydrogen: Scaling up to meet city transportation demands," *Int. J. Hydrogen Energy*, vol. 39, no. 28, pp. 15570–15582, 2014.
[26] J. Qiu *et al.*, "Multi-Stage flexible expansion co-planning under uncertainties in a combined electricity and gas market," *IEEE Trans. Power Syst.*, vol. 30, no. 4, pp. 2119–2129, Jul. 2015.
[27] J. Fang, Q. Zeng, X. Ai, Z. Chen, and J. Wen, "Dynamic optimal energy flow in the integrated natural gas and electrical power systems," *IEEE Trans. Sustain. Energy*, vol. 9, no. 1, pp. 188–198, Jan. 2018.
[28] The Advanced Research Projects Agency Energy, "Duration addition to electricity storage (DAYS) overview," 2018. [Online]. Available: https://arpa-e.energy.gov/technologies/programs/days
[29] U.S.Department of Transportation, "2017 National Household Travel Survey," 2017. [Online]. Available: https://nhts.ornl.gov/
[30] K. Forrest, M. Mac Kinnon, B. Tarroja, and S. Samuelsen, "Estimating the technical feasibility of fuel cell and battery electric vehicles for the medium and heavy duty sectors in California," *Appl. Energy*, vol. 276, 2020, Art. no. 115439.
[31] G. Pareschi, L. Küng, G. Georges, and K. Boulouchos, "Are travel surveys a good basis for EV models? Validation of simulated charging profiles against empirical data," *Appl. Energy*, vol. 275, 2020, Art. no. 115318.
[32] U.S. Department of Energy and Alternative Fuels Data Center, "Vehicle Weight Classes and Categories," 2015. https://afdc.energy.gov/data/10380
[33] S. Samuelsen, B. Shaffer, J. Grigg, B. Lane, and J. Reed, "Performance of a hydrogen refueling station in the early years of commercial fuel cell vehicle deployment," *Int. J. Hydrogen Energy*, vol. 45, no. 56, pp. 31341–31352, 2020.
[34] P. Denholm and M. Hand, "Grid flexibility and storage required to achieve very high penetration of variable renewable electricity," *Energy Policy*, vol. 39, no. 3, pp. 1817–1830, 2011.
[35] Y. Xu *et al.*, "U.S. Test system with high spatial and temporal resolution for renewable integration studies," in *Proc. IEEE Power Energy Soc. General Meeting*, 2020, pp. 1–5.
[36] Maxwell Brown, W. Cole, E. Kelly, J. Becker, D. Bielen, and I. Chernyakhovskiy, "Regional Energy Deployment System (ReEDS) Model Documentation," Colorado, 2017. [Online]. Available: https://www.nrel.gov/analysis/reeds/
[37] U.S. Energy Information Administratioin, "Form EIA-860," 2020. [Online]. Available: https://www.eia.gov/electricity/data/eia860/
[38] Electric Reliability Council of Texas, "Resource Adequacy," 2019. [Online]. Available: http://www.ercot.com/gridinfo/resource
[39] U.S. Department of Energy, "Hydrogen and Fuel Cell Technologies Office Multi-Year Research, Development, and Demonstration Plan," 2016. [Online]. Available: https://www.energy.gov/eere/fuelcells/downloads/hydrogen-and-fuel-cell-technologies-office-multi-year-research-development
[40] U.S. Department of Energy, "Manufacturing Cost Analysis of 100 and 250 kW Fuel Cell Systems for Primary Power and Combined Heat and Power Applications," 2016. [Online]. Available: https://www.energy.gov/sites/prod/files/2016/07/f33/fcto_battelle_mfg_cost_analysis_pp_chp_fc_systems.pdf
[41] International Energy Agency, "The Future of Hydrogen," 2020. [Online]. Available: https://www.iea.org/reports/the-future-of-hydrogen
[42] National Renewable Energy Laboratory, "2020 Annual Technology Baseline," 2020. [Online]. Available: https://atb.nrel.gov/
[43] Bureau of Transportation Statistics, "Number of U.S. Aircraft, Vehicles, Vessels, and Other Conveyances," 2020. [Online]. Available: https://www.bts.gov/content/number-us-aircraft-vehicles-vessels-and-other-conveyances
[44] U.S. Environmental Protection Agency, "Automotive Trends Report," 2020. [Online]. Available: https://www.epa.gov/automotive-trends/highlights-automotive-trends-report
[45] Commercial Truck Trader, "Commercial truck trade", 2021. [Online]. Available: http://www.commercialtrucktrader.com/
[46] U.K Goveronment, "The 2050 Calculato," 2013. [Online]. Available: http://2050-calculator-tool.decc.gov.uk/#/home
[47] U.S. Department of Energy, "Fuel economy information," 2015. [Online]. Available: https://www.fueleconomy.gov/
[48] E. S. Hecht and J. Pratt, "Comparison of conventional vs. modular hydrogen refueling stations, and on-site production vs. delivery," Natl. Renew. Energy Lab. U.S. Dep. Energy., 2017, [Online]. Available: https://www.energy.gov/sites/prod/files/2017/03/f34/fcto-h2first-reference-station-phase2-2017.pdf
[49] International Energy Agency, "Global EV Outlook 2019," 2019. [Online]. Available: https://www.iea.org/reports/global-ev-outlook-2019
[50] Michael Nicholas, "Estimating electric vehicle charging infrastructure costs across major U.S. metropolitan areas," 2019. [Online]. Available: https://theicct.org/publications/charging-cost-US
[51] M. Nicholas, D. Hall, and N. Lutsey, "Quantifying the electric vehicle charging infrastructure gap across U.S. markets," *Int. Counc. Clean Transp.*, 2019, [Online]. Available: https://theicct.org/publications/charging-gap-US
[52] The California Department of Transportation, "California Household Travel Survey," 2015. Accessed: Jan. 14, 2021. [Online]. Available: https://www.txdot.gov/inside-txdot/division/transportation-planning/travel-survey.html
[53] M. Arbabzadeh, R. Sioshansi, J. X. Johnson, and G. A. Keoleian, "The role of energy storage in deep decarbonization of electricity production," *Nat. Commun.*, vol. 10:3413, 2019, doi: 10.1038/s41467-019-11161-5

Bo Li (Student Member, IEEE) received the B.S. degree in electrical engineering from Guangxi University, Nanning, China, in 2016. He is currently working toward the Ph.D. degree with Chongqing University, Chongqing, China.

His major research interests include power system optimization and planning, energy policy, and renewable energy integration.

Minyou Chen (Senior Member, IEEE) received the M.Sc. degree from Chongqing University, Chongqing, China, in 1987, and the Ph.D. degree in automatic control and systems engineering from the University of Sheffield, Sheffield, U.K., in 1998.

He is a Professor of electrical engineering with the School of Electrical Engineering, Chongqing University. His main research interests include intelligent modeling and control, multi-objective optimization, smart grid, and reliability of power electronic equipment.

Ziming Ma (Member, IEEE) received the B.S. and Ph.D. degrees in electrical engineering from Tsinghua University, Beijing, China, in 2015 and 2020, respectively.

He is currently with the National Power Dispatch and Control Center, State Grid Corporation of China. His research interests include power system operations and electricity markets.

Gang He received B.S. degree and M.A. degree in geography from Peking University, Beijing, China, in 2003 and 2006. He received M.A. degree in climate and society from Columbia University, New York, NY, USA, in 2008, and the Ph.D. degree in energy and resources from University of California at Berkeley, Berkeley, CA, USA, in 2015.

He is currently an Assistant Professor with the Department of Technology and Society, Stony Brook University, Stony Brook, NY, USA. His research interests include energy modeling, energy economics, energy and climate policy, energy, and environment.

Wei Dai (Member, IEEE) received the Ph.D. degree in electrical engineering from Chongqing University, Chongqing, China, in 2018.

He is currently an Assistant Professor with Guangxi University, Nanning, China. His research interests include multiple energy systems, power systems analysis, renewable energy, and large-scale system problems.

Dongran liu received the B.S. degree in economics and management from North China Electric Power University, Baoding, China, in 2015. She is currently working toward the Ph.D. degree with North China Electric Power University, Beijing, China.

Her major research interests include electricity market, bidding strategies, energy storage, and energy market.

Chi Zhang (Student Member, IEEE) received the Ph.D. degree in electrical engineering from Chongqing University, Chongqing, China, in 2021.

Haiwang Zhong (Senior Member, IEEE) received the B.S. and Ph.D. degrees in electrical engineering from Tsinghua University, Beijing, China, in 2008 and 2013, respectively.

He is currently an Associate Professor with the Department of Electrical Engineering, Tsinghua University. His research interests include smart grids, power system operations, electricity markets, and demand response.